Arab American University

Faculty of Graduate Studies

Department of Health Sciences

Master Program in Computed Tomography and MRI Science

Comparing Arterial Virtual Non-Contrast Scans with Venous Virtual Non-Contrast Scans in Their Feasibility to Substitute True Non-Contrast Scans Using Detector-Based Spectral Computed Tomography Scanner

Manar Mohammad Mahmoud AL-Qaisi
202113094

Supervision Committee:

Dr. Abed-AL Salam Ahmad Abed Khalaf

Dr. Ahmad Rafeeq Abu Arrah

Dr. Osama Ali Khodrog

This Thesis was Submitted in Partial Fulfillment of the Requirements for the Master Degree in Computed Tomography and Magnetic Resonance Imaging Science.

Palestine, 05/2025

Arab American University

Faculty of Graduate Studies

Department of Health Science

Master Program in Computed Tomography and MRI Science

Thesis Approval

Comparing Arterial Virtual Non-Contrast Scans with Venous Virtual Non-Contrast Scans in Their Feasibility to Substitute True Non-Contrast Scans Using Detector-Based Spectral Computed Tomography Scanner

Manar Mohammad Mahmoud AL-Qaisi
202113094

This thesis was defended successfully on 12/5/2025 and approved by:

Thesis Committee Members:

Name	Title	Signature
1. Dr. Abed-AL Salam Khalaf	Main Supervisor	
2. Dr. Ahmad Rafeeq Abu Arrah	Member of Supervision Committee	
3. Dr. Osama Ali Khodrog	Member of Supervision Committee	

Palestine, 05/2025

Declaration

I declare that, except where explicit reference is made to the contribution of others, this thesis is substantially my own work and has not been submitted for any other degree at the Arab American University or any other institution.

Student Name: Manar Mohammad Mahmoud AL-Qaisi
Student ID: 202113094
Signature: Manar Mohammad AL-Qaisi
Date of Submitting the Final Version of the Thesis: 27/7/2025

Dedication

In the name of Allah, most gracious most merciful

This dissertation is dedicated to my mother, my father, my brothers, and my sisters, who although they were initially not happy with the idea of me continuing my education postgraduate, still supported my dreams and encouraged me at every step along the way.

This study also goes to my friends and classmates that I met during my master journey, since if it was not for them, I could have lost my way in the middle of the road.

Manar Mohammad Mahmoud AL-Qaisi

Acknowledgements

This work would not have been possible without the help of a lot of people. For a starter, I would like to thank Dr. Abed-AL Salam Khalaf for his guidance throughout this whole study; I would also like to thank all my teachers at the Arab American University, every small piece of advice has been a great help in this journey.

All my gratitude to my family and friends, for whenever I stumble down and fall, they pick me up from the ground and help me keep going.

This study would not have been possible without the help of all the staff from the radiology department in AL-Rahma clinic, in particular, I would like to mention Zaid Daraghmah for helping me with every part of the methodology, from the data collection to the imaging parameters and set-up, for that, I would like to give you my full gratitude and appreciation.

Lastly, I would like to thank all the people who, although I may have not mentioned them, have been a big help and support throughout my educational journey.

Comparing Arterial Virtual Non-Contrast Scans with Venous Virtual Non-Contrast Scans in Their Feasibility to Substitute True Non-Contrast Scans Using Detector-Based Spectral Computed Tomography Scanner

Manar Mohammad AL-Qaisi

Supervision Committee:

Dr. Abed-AL Salam Ahmad Abed Khalaf

Dr. Ahmad Rafeeq Abu Arrah

Dr. Osama Ali Khodrog

Abstract

Introduction: Spectral Computed Tomography (CT) is one of the innovations in radiology that has helped reduce the patient's dose and improve the image quality; one of the applications that can be done using spectral CT is the creation of Virtual Non-Contrast (VNC) images using material decomposition, these images can be created from any phase in contrast-enhanced scans. If VNC images closely resemble True Non-Contrast (TNC) images, TNC images can be replaced with VNC images and reduce the patient dose.

Purpose: This study aims to compare VNC images created from the arterial phase (VNC-A) and the VNC images created from the venous phase (VNC-V) with the TNC images for the abdomen, to determine if either of them is similar to the TNC image enough to replace it.

Methods: 141 abdominal CT scans, which were done in AL-Rahma clinic between July 2022 and October 2024 using a detector-based spectral CT scanner, were enrolled in the study; each scan had a non-enhanced phase, an arterial-enhanced phase, and a venous-enhanced phase. A VNC image was reconstructed from both the venous phase and the arterial phase, and the images were compared by the Mean Attenuation (MA) and the Standard Deviation (SD) of the Regions Of Interest (ROI) that were placed in five different places across the abdomen, to show the difference between the images in term of the attenuation values and the image noise.

Results: The relation between the TNC with VNC-A images, and TNC with VNC-V images across all ROIs was significantly different, with TNC having higher mean MA values (46.36 for TNC in comparison to 39.87 for VNC-A and 34.66 for VNC-V in ROI (2)), and SD values (19.27 for TNC in comparison to 10.45 for VNC-A and 10.34 for VNC-V in ROI (5)) than both VNC image types. The Signal-to-Noise Ratio (SNR) was also higher in TNC than that in VNC-A and VNC-V.

Conclusion: Neither VNC-A nor VNC-V were sufficient to replace TNC images without degrading the image quality and the diagnostic ability of the scan, due to significant differences in the attenuation numbers and the SNR.

Keywords: Spectral CT, Virtual Non-Contrast, True Non-Contrasts, VNC-A, VNC-V.

Table of Contents

List of Tables

List of Figures

List of Appendices

List of Definitions of Abbreviations

Abbreviations	Title
AAUP	Arab America University of Palestine
AEC	Automatic Exposure Control
ALARA	As Low As Reasonably Achievable
CNR	Contrast-to-Noise Ratio
CT	Computed Tomography
CTDI	Computed Tomography Dose Index
DLP	Dose Length Product
FBP	Filtered Back Projection
FOV	Field Of View
HU	Hounsfield Unit
IRB	Institutional Review Board
ISP	IntelliSpace Portal
kVp	kilo-Voltage peak
LET	Linear Energy Transfer
MA	Mean Attenuation
mA	milliAmpere
PET/CT	Positron Emission Tomography with Computed Tomography
ROI	Region Of Interest
SD	Standard Deviation

SNR	Signal-to-Noise Ratio
SPSS	Statistical Package for Social Sciences
TNC	True Non-Contrast
VMI	Virtual Mono-energetic Image
VNC	Virtual Non-Contrast
VNC-A	Virtual Non-Contrast from the Arterial phase
VNC-V	Virtual Non-Contrast from the Venous phase

Chapter One: Introduction

1.1 Background

Computed Tomography (CT) has been an essential diagnostic imaging modality for decades now; it has become an irreplaceable source for observing the human anatomy substituting the need for many invasive and high-risk procedures such as ventriculogram and pneumoecephalography (Schulz, Stein and Pelc, 2021); in addition, the CT scan's efficiency has increased after its introduction of multi-phasic imaging using a contrast material to better visualize low-contrast tissues from one another, which can be especially helpful in the abdomen where several organs and soft tissues with similar attenuation coefficients exist (Menon *et al.*, 2015; Dundamadappa *et al.*, 2021; Wang *et al.*, 2021).

Individual institutions with different CT scanners have different acquisition's parameters and protocols for imaging the patient a multi-phasic scan, but the scan normally consist of a non-enhanced image as well as contrast-enhanced images taken in different phases such as the arterial phase and venous phase; in some cases, a delay phase may be obtained depending on the purpose of the CT scan and the patient's medical condition.

Each of these phases contains information that can be helpful in patient diagnosis and is therefore essential. Although the non-enhanced phase doesn't help visualize low-contrast organs from one another, it is still important since it acts as a basis for the quantification of contrast uptake and can also provide benefits for critical decision-making since the presence of the contrast material could be masking an integral part of the image, such as in the detection of intramural hematoma (Kelly *et al.*, 1989; Payor *et al.*, 2015; Mussa *et al.*, 2016; Li *et al.*, 2018).

The problem starts to unfold with the fact that scanning the patient multiple phases during one scan will increase the overall patient's radiation dose as well as the risk probability of getting radiation-induced cancer, to the point where many institutions' protocols exclude the non-enhanced scan despite its value in the patient's diagnosis and

decision-making, and since the patient dose is a major problem in CT, multiple ways have been suggested to find a way to omit the need for one acquisition without reducing the scan's diagnosis accuracy which can be extremely helpful as it will reduce the patient dose significantly (Shah, Sachs and Wilson, 2012).

With the increase of CT examinations worldwide, the need to reduce the patient dose during imaging became higher, in 2020, approximately 300 million CT scans per year were done with a 4% increase in numbers per year (Schöckel *et al.*, 2020). Many solutions and ways have been suggested and applied to decrease the patient dose that falls under the general principle of radiation safety which suggests that the radiation dose used should be As Low As Reasonably Achievable (ALARA).

Example for some of these solutions that have been applied to reduce the patient dose includes the use of tube current modulation that can be used on both the X-Y axis and the Z-axis and the use of the Automatic Exposure Control (AEC) to adjust the dose based on the thickness of the body part that is being imaged (McCollough *et al.*, 2009).

As mentioned earlier, one way to reduce the patient dose is by decreasing the number of scans needed to obtain an accurate diagnosis, taking into account that the effective dose for one abdomen-pelvis scan is about 10 mSv (Smith-Bindman, 2009; Sulieman *et al.*, 2022), for a multi-phasic exam this number will be doubled certain times based on the number of acquisitions needed. If the need for one of these acquisitions was omitted without reducing the diagnostic ability and accuracy of the exam, the patient dose will significantly decrease.

Spectral CT is one of the innovations in radiology that has benefited image quality and dose reduction; the principle to generate spectral images is to have two different energy levels or energy spectra in the photons that create the image. This can be done in multiple ways; for example, by having two radiation sources or one radiation source that switches the tube potential rapidly.

These types of scanners can create both spectral images and can also create conventional CT images if the scanner has used only one radiation source during imaging out of the two. If the system was pre-requested to collect spectral data, the radiation source or sources will produce photons with dual-energy spectra and spectral images will be created,

if no request was made the spectral data will not be available, which means that the creation of spectral images is not automatic and has to be pre-requested.

Another type of spectral CT system that can solve the problem of pre-requesting the spectral data is the detector-based spectral CT scanner, this scanner uses only one radiation source with a poly-energetic beam and has a dual-layer scintillator type detector in which the first layer absorbs the low-energy photons creating a low-energy image, and the second layer absorbs the high-energy photons that penetrate the first layer and create a high-energy image simultaneously with the creation of the low-energy image, both images are then added together creating a spectral image that is automatically generated in all scans without the need to adjust the imaging parameters prior to the acquisition (McCollough *et al.*, 2015).

This type of scanner has many benefits, since, as we mentioned earlier it doesn't require pre-requesting for the spectral data to be acquired, giving spectral images for all the scans of the patient. Another benefit of this type of scanner is that it delivers the same amount of radiation as the conventional single-source CT scanner, so the spectral data is acquired without increasing the patient dose (Hua *et al.*, 2018).

A Virtual Non-Contrast (VNC) image is an image created by a post-processing technique using spectral CT, since spectral CT can generate material-decomposition data, we can identify the iodine voxels, which represent the contrast material, in the image and remove them creating, by that, an image without contrast material enhancement from a contrast-enhanced image without the need to scan the patient an additional scan (Sauter *et al.*, 2018).

VNC images can be taken from contrast-enhanced scans in any phase of imaging, whether it's from the arterial phase, venous phase, or even the delayed phase, an iodine map can be created from the original enhanced image and subtracted from it, this way we can make a non-enhanced image without the need to scan the patient another time, and if the virtual image was closely resembling the truly non-enhanced image in terms of the attenuation values and the image quality, the need for the non-enhanced phase will be omitted and this technique will reduce both the patient's dose and the scan time (McCollough *et al.*, 2015).

Many studies have been conducted to search the feasibility of using VNC images instead of True Non-Contrast (TNC) images in a number of different medical cases, reducing the time of the scan and more importantly, the patient dose; in most studies, the CT numbers on both images were either significantly close to deem VNC images an acceptable alternative to the TNC images in the study's medical case, or that the difference was negligible and the VNC image's results were deemed sufficient to replace TNC images (Kaufmann *et al.*, 2013; Slebocki *et al.*, 2017).

It is worth noting that in these studies the VNC images are usually taken from one phase only, either from the arterial phase or the portal-venous phase, thus, not from multiple phases to decide which one will give the most resemblance to the TNC images' attenuation values and image quality.

This study aims to compare and test the feasibility of replacing the TNC images with VNC images in abdominal scanning to reduce the patient's dose and scan time without compromising on the image quality and diagnostic ability using a detector-based spectral CT scanner, and to determine which of the arterial-phase derived VNC image (VNC-A) and the venous-phase derived VNC image (VNC-V) is more similar to the TNC image in terms of attenuation values and image noise to give more accurate results.

1.2 Statement of the Problem

With the increased use of CT imaging as a diagnostic tool in different medical applications (Schöckel et al., 2020), the radiation dose will also increase, which results in higher chances of the patient's risk of acquiring radiation-induced cancer (Shah, Sachs and Wilson, 2012). Therefore it will be helpful to find a way to reduce patient exposure to radiation; one suggested way is by decreasing the number of acquisitions needed for multi-phasic imaging without reducing the scan's diagnosis ability.

Meanwhile, spectral CT has made it possible to create images that appear free of contrast material enhancement and are generated from contrast-enhanced images using material decomposition; these are called VNC images (Rassouli *et al.*, 2017). Some scans require imaging the patient in multiple phases including a scan without contrast and both

arterial and venous phase scans with contrast media enhancement. If VNC images driven from either the arterial or venous phases were sufficient to replace TNC images without degrading the image quality and diagnostic ability, this could help reduce the patient dose and the time needed in the scanning room.

1.3 Objectives of the Study

The main objective of this study is to compare VNC images driven from the arterial phase of contrast-enhanced images and VNC images driven from the venous phase of contrast-enhanced images with TNC scans in order to find which one of them would be a more accurate replacement for TNC images in abdominal scans.

Sub-objectives: To test the feasibility of using VNC images instead of TNC.

1.4 Study Hypothesis

- VNC images can be used as an alternative to TNC images in studies that require high CT number accuracy in abdominal imaging.
- VNC images based on the venous phase are more similar to the TNC images than the VNC images based on the arterial phase in terms of CT number accuracy.

1.5 Study Questions

Which VNC image is more similar to the TNC image in terms of CT number accuracy, VNC images based on the arterial phase or VNC images based on the venous phase?

Sub-questions:

-Can VNC images derived from either the arterial phase or the venous phase replace TNC images in abdominal scans?

-How different are the CT number readings from arterial VNC images and venous VNC images in comparison to the TNC images?

-How different is the image quality between the arterial VNC images and the venous VNC images in comparison to the TNC images?

1.6 Significance of the Study

Many CT scans require imaging the patient both with and without contrast media enhancement which exposes the patient multiple times to ionizing radiation and increases the patient's risk of getting radiation-induced cancer, finding a way to create both images without reducing the image quality and its diagnostic accuracy and without imaging the patient multiple times and exposing the patient to extra radiation dose could be helpful as it results in significant reduction in the patient dose and the time spent in the scanner room as well.

And when exposing the patient to higher doses of radiation, the risk of radiation-induced cancer will increase, that is why finding ways to decrease the patient dose without decreasing the diagnostic ability of the image is crucial. One way to reduce the patient dose is by eliminating the need for a certain acquisition by replacing it with an alternative option that doesn’t require exposing the patient to more ionizing radiation.

If the spectral VNC images created from either the arterial or venous phase were similar to TNC images in terms of the attenuation number and the image quality, they could substitute the need for an additional TNC scan, resulting in reducing the patient’s exposure to radiation and spending less time in the scanner room. Finding out which of the two VNC images is more similar to the TNC image will help in giving more accurate results when replacing the TNC images without comprehending the image quality or diagnostic ability.

1.7 Outline the Structure of the Study

The structure of the study and its findings will be arranged as the following:

Chapter One: Introduction

1.1 Introduce the general concepts of the study.

1.2 Define the study's problem.

1.3 Determine the aims and objectives of the study.

1.4 Formulate the thesis questions and hypotheses.

1.5 State the significance of the study.

Chapter Two: Literature Review

2.1 Explore the key points and the research topics related to the study, including CT's recent developments and clinical applications, risks of the patient's radiation dose, and the most common ways to reduce it, as well as spectral CT, material decomposition, and VNC imaging.

2.2 Discuss the results of the studies that were previously conducted around this research topic.

2.3 Explain the gap in the literature around the research subject.

Chapter Three: Methodology

3.1 Introduce the study design and setting.

3.2 Explain the ethical considerations regarding the study.

3.3 Determine the study population and the inclusion and exclusion criteria.

3.4 Explain the methods used in the study including data collection and image analysis.

3.5 Stating the statistical analysis conducted on the data.

Chapter Four: Results

4.1 Presenting the findings of the study.

4.2 Explaining the data analysis related to the study's questions and theories.

Chapter Five: Discussion and Conclusion

5.1 Discuss the results of the study and compare them to the results of previous studies conducted on similar topics.

5.2 Conclude the results of the study.

5.3 Point out the strengths and the limitations of the study.

5.4 Give recommendations regarding the results obtained from the study.

5.5 Suggesting future work that needs to be done that can help this study.

Chapter Two: Literature Review

2.1 Introduction

This chapter will discuss what the literature has studied and found about CT scanners, multi-phasic imaging, patient dose, and potential risks of radiation, as well as discuss spectral CT, material decomposition, and VNC images. It will also bring light to previous studies that were conducted to test the feasibility of using VNC images instead of TNC images and all the information that was studied and concluded about the current study.

The literature that was utilized to write this section included articles that were collected from PubMed, Science Direct, Google Scholar, and white papers from trusted websites for marketing organizations, as well as books and textbooks that are related to the topics of the current study.

2.2 Computed Tomography Background

CT is an essential tool in health care and medical imaging and it's among the main instruments used for patients' diagnosis. The first clinical CT scanner prototype emerged in 1971 and the first patient was scanned in 1972, since then with the rapid advances of computers and technologies, the clinical developments and improvements of the CT scanners and the design of the x-ray tube advanced alongside them. These developments were focused on multiple needs to optimize the scanning procedure, such as faster acquisitions, higher image quality, lower tube heat, and reduced patient dose.

The principle of CT imaging is based on the idea that when an X-ray beam passes through a material and collected on the other side with a detector, we can obtain information about that specific material since the X-ray beam will be attenuated by an amount based on the material thickness and atomic number, and if the X-ray passes through the human body with certain energy from multiple directions, an image containing information about the body

structure in three dimensional (3D) representation could be produced by the detector that was placed at the end of the beam.

This was a big breakthrough and change from the two dimensional (2D) images that were the only imaging tool available in the medical field. When an X-ray photon with certain energy interacts with the patient's body, the photon is attenuated by an amount that depends on the density of the structure and its atomic number, this attenuation coefficient is different for each material depending on its physical properties (Seeram and Sil, 2013).

So different materials give different attenuations that are translated differently on the image based on the X-ray linear attenuation coefficient and assigned the correct Hounsfield Unit (HU) therefore, a grey-scale shadow will be assigned for the tissue so that it can be distinguished from other materials with different attenuation coefficient, the HU is calculated for each material based on their attenuation coefficient in relation to the water attenuation coefficient, and it can be calculated as follows.

$$HU = \frac{\mu_{tissue} - \mu_{water}}{\mu_{water}} \times 1000 \qquad (1)$$

Knowing that μ_{tissue} is the attenuation coefficient for the tissue that the HU is being calculated for, μ_{water} is the attenuation coefficient for the water, and 1000 is a consent that represents the contrast factor, which means that the HU range is from -1000, which is for air, and +1000, which is for bone (Seeram and Sil, 2013). The difference in the attenuation coefficient between the tissues is what creates the CT image and make it useful in multiple clinical applications.

2.3 CT Uses in Medical Applications

The developments in CT scanners have made them the golden standard diagnostic tool in many medical applications, at the beginning of the spread of CT scanners in hospitals and clinics it was only used to locate and distinguish suspected lesions in the patient's body, since then, CT has found its way in multiple other applications such as angiography, CT fluoroscopy, simulation in radiation therapy, portable CT imaging, quantitative CT, CT screening, and medical image fusion (Seeram and Sil, 2013).

The use of CT in these applications was possible due to the rapidly evolving technologies in scanner production, and with the non-stop advances in these technologies, CT has a promising impact on multiple other clinical applications (Schena *et al.*, 2015). Mentioned here are examples of emerging applications for CT that recent research is focusing on developing.

CT thermometry, which can be used as a non-invasive method that gives indirect detailed thermal information from a slice of a CT scan based on the CT attenuation values, using the fact that the attenuation values for biological tissues are dependent on their temperature, this can be used to visualize the temperature of a certain organ or tissue to assess the effect of a certain procedure on them (Fani *et al.*, 2014).

Another example of CT's recent clinical applications is CT-guided procedures; this method uses CT images to guide either a diagnostic procedure such as taking a biopsy or a therapeutic procedure such as collecting aspiration from the plural cavity. CT-guided procedures have reduced the need for invasive procedures that hold a higher-risk probability for the patients.

Multiple extensions have been installed in the CT scanners to ensure that CT-guided procedures are done with most efficiency and least radiation dose possible for the patient and the medical team, such extensions include hardware extensions such as a monitor and a number of radiation protection screens that are located at the CT table, as well as some software extensions that allow advanced image reconstruction and real-time viewing of the image (Roman *et al.*, 2018).

Hybrid Positron Emission Tomography/CT (PET/CT) is another recent innovation that was made possible due to the advances in CT technology, hybrid imaging allows to benefit from both imaging technique to optimize the efficiency of the scan, especially in tumor imaging and staging, CT images can map the morphology of the tumor and provide anatomical information, while performing PET can give information about the tumor metabolism, both of these types of information is critical during treatment planning and follow-up to check the tumor response for the treatment (Kapoor, McCook and Torok, 2004).

Phase-contrast Imaging was essentially used in microscopy, first using visible light and then using X-ray, and with the advancements in technology, it was possible to create phase-contrast images with edge enhancement to differentiate between materials with similar densities, such as the internal organs, these images depend on the X-ray refraction as it passes through the material instead of the photon absorption, this technique has showed some promising results in the literature (Tapfer *et al.*, 2012).

The use of photon-counting detector in spectral CT was a groundbreaking technique that has been possible due to the rapid advancements in X-ray technology, the photon-counting detectors can count each single photon that reaches it and measure its energy, and with that knowledge, spectral images taken with multiple X-ray energy spectra can be developed and used to generate material decomposition information (Meloni *et al.*, 2024).

2.4 Multi-Phasic Imaging

For certain imaging procedures, the need to enhance the visibility of certain tissues is crucial in the diagnosis process since multiple organs and tissues in the body have similar densities, for example, muscles in the patient's body have a similar attenuation coefficient to the blood and they appear similar on the CT image with very little contrast between them.

Iodinated-based contrast material is used to differentiate low-contrast organs and tissues from one another, using intravenous contrast material allows the material to pass through the arteries, the veins, and certain tissues and organs within the patient's body and make them more visible (Costa, 2004). If the scan was acquired while the contrast media was passing through the artery, the phase of imaging will be called the arterial phase, different phases with different timings are required for each patient depending on their case.

During a multi-phasic CT scan of the abdomen, a non-enhanced scan will first be taken followed by the arterial phase, venous phase, and in some cases, a delayed phase that might be a single scan or sometimes more, each of these phases is essential and will carry some type of information regarding the patient’s condition based on the location of the contrast media in the patient’s body, and numerous studies have showed the role of multi-

phasic CT in the detection and diagnosis of multiple clinical cases (Foley *et al.*, 2000; Zhao, 2003; Menon *et al.*, 2015).

The non-enhanced phase is as necessary as the enhanced phases, although multiple institutions excluded it from the scan to reduce that patient dose, these scans might not reach their full diagnosis capability without the presence of the unenhanced phase, as it allows the visualization of structures that might be obscured by the contrast media in the enhanced phases, such as calcifications or stones, and this might be critical in many situations such as in the detection of intramural hematoma, additionally, multiple other clinical cases use the unenhanced phase as a base for quantifying the uptake of contrast media in certain organs and tissues (Kelly *et al.*, 1989; Payor *et al.*, 2015; Mussa *et al.*, 2016; Li *et al.*, 2018).

2.5 CT Radiation Dose and its Risks

One of the disadvantages of multi-phasic CT scans is increasing the patient dose, since the patient is scanned several times the total CT Dose Index (CTDI) and the Dose Length Product (DLP) will significantly increase compared to mono-phasic scans. The patient dose is an issue that is continuously being studied for fear of the risks and the long-term effects it has on the body (Shah, Sachs and Wilson, 2012), the biological effects of low Linear Energy Transfer (LET) radiation, that is being used in the medical field, have been studied and its risks have been estimated since the Japanese atomic bomb in 1945 (Hunter and Muirhead, 2009).

The biggest health risk of low-LET radiation is radiation-induced cancer, which has a linear relationship with the radiation dose at low- and medium-energy levels, as can be seen in (Fig 2.1), from this it was concluded that exposing the patient to higher doses of radiation, such as in multi-phasic imaging, will increase the risk of radiation-induced cancer (Brenner *et al.*, 2003).

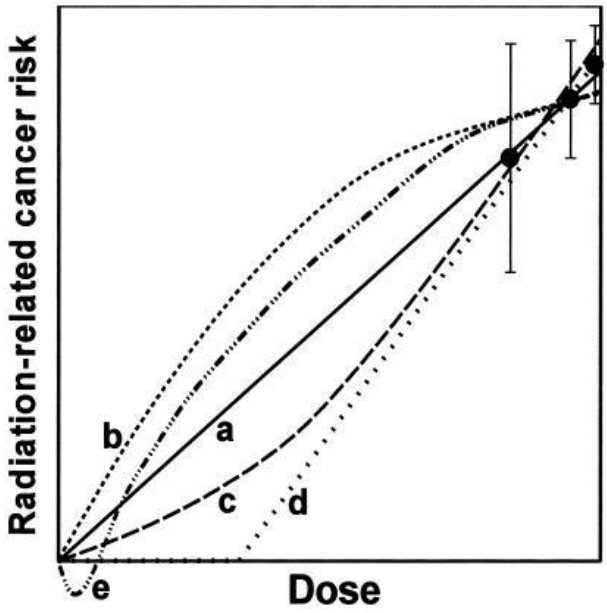

Figure 2.1: Schematic Representation of Different Possible Extrapolation of Measured Radiation Risk Down to Very Low Doses.

2.6 Radiation Dose Reduction Methods

The widespread use of CT imaging and the increase in numbers of scans have led researchers to focus on finding methods to reduce the patient dose and the possible risks associated with it, numerous studies have tested dose reduction techniques and their efficiency in decreasing the patient dose without compromising the image quality (McCollough *et al.*, 2009; Marin *et al.*, 2011; Hara *et al.*, 2013).

Taking into account the patient size during imaging and selecting the parameters, specifically, the tube current in milliAmpere (mA), can play a crucial role in reducing unnecessary doses to the patient. Recent scanners have deployed the use of AEC and tube current modulation in CT scans; this can change the mA of a projection depending on the density of the material it will pass through, and it is possible to use this technique in both the X-Y axis of the scan and the Z-axis of the scan (Graser *et al.*, 2006).

Reducing the kilo-Voltage peak (kVp) can also work to reduce the patient's dose, most scanners have a set of 120kVp but it can be adjusted to 100kVp or even 80kVp in some

situations such as when imaging certain contrast-enhanced scans, this technique has been studied and proven to be beneficial since the image contrast is heightened in the contrast-enhanced scan and the tissue visibility of the image will not be reduced even with the decreased kVp, this way the patient dose will be significantly reduced without degrading the image quality (Takahashi *et al.*, 2018).

Another way to reduce the patient's dose is by using a filter to reduce the scatter radiation as well as the image noise, with the image noise decreased the scanning parameters can be lowered without worrying about the quality of the image, and reducing the scatter radiation will also decrease the unwanted dose entering the patient's body without taking part in the image production. The most common types of filters that are used in CT are the bow-tie filter and most recently the tin filter (Anam, 2020; Greffier *et al.*, 2020).

Reducing the noise can also be accomplished by applying iterative reconstruction algorithms which, unlike the standard Filtered Back Projection (FBP) algorithm, can filter the noise from the projection data and give a higher quality image without increasing the patient's dose (Mohammadinejad *et al.*, 2021).

2.7 The Developments and Innovations in CT Scanners

Recent developments in CT scanner technology focus on increasing the image quality, decreasing the patient dose, and reducing scanning time. Such innovations are being introduced to this day; for example, recently in 2020 the University collage of London introduced the concept of cycloidal CT where images are generated by using thin beamlets that aim to produce a higher in-slice spatial resolution to the image despite the use of relatively bigger focal spot and detector pixels.

The use of beamlets is to produce an image without any significant overlap between the beamlets which increases the spatial resolution and image quality, and during a preliminary study it was discovered that the Signal-to-Noise Ratio (SNR) is higher in the images in comparison with the dose delivered (Hagen *et al.*, 2020).

New technologies have also led to the development of faster CT scanners that offer to scan the patient's heart within milliseconds using a cone-shaped X-ray beam and the introduction of 64-slice CT has led to a 128-slice CT, 256-slice CT, and most recently 640-slice CT to widen the scan length taken in one gantry rotation. These scanners are crucial when imaging the heart and the coronary artery which is subjected to an uncontrollable motion artifact if it was not imagined in a short frame of time especially for patients with higher heart rates or heart arrhythmia (Cao *et al.*, 2019).

As mentioned earlier the use of the iterative reconstruction algorithm, which has been a break-through technical innovation in dose reduction, has been replacing the basic FBP algorithm, this algorithm is a process that produces a higher quality CT image with reduced patient dose, this technique is done mathematically by starting with an image assumption, this image is then adjusted constantly based on the data of the image that is being taken until it reaches its final form (Stiller, 2018).

Recent advances in technology have also led to the development of one of the most promising emerging scanners not only in terms of increasing image quality and in patient dose and scan time reduction but also, in introducing CT as a diagnosis tool in multiple clinical applications that CT was not part of in the past, that is the spectral CT scanner.

2.8 Spectral CT Imaging

As previously mentioned, the principle of generating CT images is by exposing the patient to single energy spectra radiation, the radiation photons then penetrate the body and get attenuated by a number that depends on the material it passed through, the photon then is received by the detector and the attenuation value will give information about the material’s type or density to produce an image set from a single X-ray energy spectrum.

The idea of spectral CT or dual-energy CT is to have two different photons' energy spectra pass through the material, and the identification of that material will depend on its K-edge, which is the energy needed to release an electron from the innermost shell or the K shell and it differs between different elements based on their atomic number, the higher the

atomic number the higher the K-edge will be for that element. The element will then interact differently when using different energies, the photons will then leave the patient body to be received by the detector on the other side of the patient holding specific material information from two different energies (Johnson, 2012; McCollough *et al.*, 2015).

In conventional scanning the photon leaving the body holds information based on the linear attenuation coefficient, the linear attenuation coefficient depends on both the photon's energy and the material it passes through, that means when, for instance, an energy spectrum of 140kVP and another of 80kVp passes through the same material the mean attenuation coefficient will differ and the exiting photons will have different attenuations and holding different information about the same material which can help delineate it (Garnett, 2020).

Using two energy levels to create an image can give us materials-specific information, based on the theory of the three materials decomposition, which are two materials with low atomic numbers and one material with a high atomic number, such as the soft tissue, the fat, and the iodine, this helps us differentiate and quantify similar materials based on their interactions with the low-energy photons and the high-energy photons.

By doing that we can generate material-decomposition images with spectral data; that can identify the different materials imaged and in return allow the creation of multiple other images such as iodine-only, effective atomic number, and virtual non-contrast images (Johnson *et al.*, 2007; Johnson, 2012; Rassouli *et al.*, 2017; Siegel, Bhalla and Cullinane, 2021).

The use of these spectral images has been studied in multiple medical applications such as the detection of endoleaks after endovascular aneurysm repair, the characterization of solitary pulmonary nodules, the staging and distinguishing between malignant and benign tumors, and the evaluation of the treatment response of the lesions (Stolzmann *et al.*, 2008; Chae *et al.*, 2010; Hong *et al.*, 2023).

2.9 Types of Spectral CT Scanner

Different types of scanners have been developed to create spectral CT images; each type has its own configuration to find a way to collect spectral data. The first type met the

need for a second energy spectrum for imaging with an additional energy source, by adding a second X-ray tube that is placed 90° offset from the first tube, the first tube will operate on low-energy potential while the second will operate on high-energy potential, two acquisitions will then be taken simultaneously, and the tubes' potentials can be pre-adjusted to count for image noise and patient dose.

One disadvantage of this type is the possibility of a slight involuntary patient motion happening during the 90° offset time between the two acquisitions, such as breathing or cardiac motion.

Another type of spectral CT scanner uses only one radiation source that is capable of ultrafast kVp switching, this way in one gantry rotation the photon potential used is alternated between high energy and low energy at an extremely fast pace. When the tube is emitting both low and high-energy photons simultaneously, two acquisitions will occur at the same time from the same angle. One limitation of this type is the fact that the tube current can't be modulated as fast as the tube potential can, and when the potential is changed from low to high, and vice versa, the current should be adjusted as well to suit the energy that was used.

Other types of spectral CT scanners also use one radiation source that switches the tube potential but the switching does not happen at ultrafast speed, the potential is switched after one gantry rotation, this way one full rotation of the tube will be done using low-energy photons and the next will be done with high-energy photons. However, this type is less preferred than the ultrafast kVp switching tube especially in cardiac and abdomen imaging, since the cardiac and lung motion could vary significantly in one full rotation of the tube.

The other type of spectral CT scanner is detector-based spectral CT which, unlike the first three types, doesn't require a pre-selection of spectral imaging, meaning that the imaging always uses high and low energies and thus, is always spectral. This type creates spectral images using a dual-layer detector; the two layers are made of different materials with different properties that allow the first top layer to absorb low-energy photons and the second bottom layer to absorb high-energy photons that penetrate the first layer, two projections are then acquired simultaneously creating two images one with only low-energy data and the second with high-energy data.

The low-energy and high-energy images are then added together to create an image from both energies with spectral data, since the two images are acquired at the same time the temporal resolution for the image is excellent which benefit the accuracy of the material decomposition. The drawback of this type is that the imaging is done based on the assumption that the first layer does not interact with the high-energy photons; if this assumption was incorrect the material decomposition might be inaccurate.

Recent spectral scanners use a special split filter that is placed in front of the tube, the filter splits the polychromatic X-ray beam into high and low energies so that during a single scan the patient will be imaged with spectral separation of the photons.

A novel type of spectral CT scanner that uses photon-counting detectors has recently been developed, the photon-counting detector has the ability to collect individual photons from the polychromatic X-ray beam and resolve it into electronic signals, creating a spectral image with more than two energies. This type is newly developed and so far has promising results with ultra-high spatial resolution. The different types of spectral CT scanner systems can be seen in Figure 2.2 (So and Nicolaou, 2021).

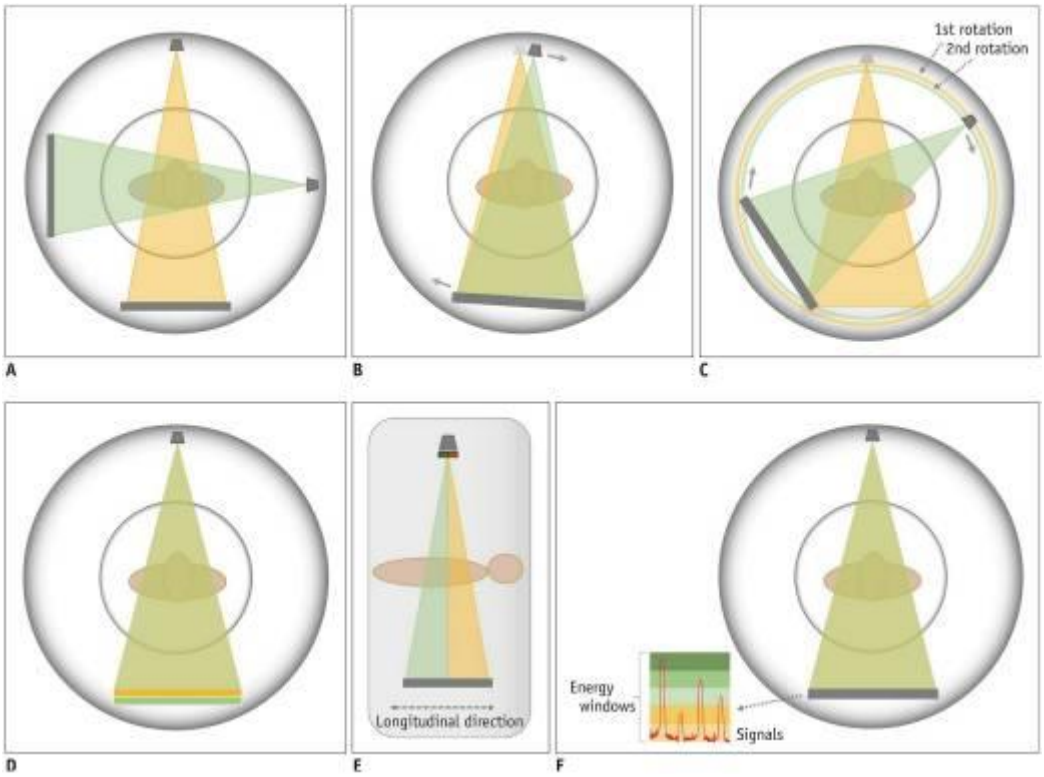

Figure 2.2: CT Scanner Systems that are Currently Available for Dual-Energy/Spectral Imaging.

A. Dual Source. B. Single Source with Ultrafast kV Switching. C. Single source without ultrafast kV switching. D. Single Source with Dual-layer detector. E. Single Source with Split Filter. F. Single Source with Photon counting detector.

2.10 Material Decomposition

The one major difference between spectral CT imaging and conventional CT imaging is the use of dual or multi-energy spectrums during image acquisition, and as stated before, having two or more energies interact with a tissue can give material-specified information that, when measured, can help differentiate it from other surrounding tissues, since spectral CT measures the response that the tissue makes based on their k-edge when exposed to different energy levels instead of only measuring the cumulative attenuation within a voxel like in conventional CT.

Within a material, two main types of photon interactions cause the material to have its own CT number in conventional CT, these are the photoelectric effect and the Compton effect, these effects are dependent on both the photon's energy and the scanned material's atomic number, the photoelectric effect has been shown to occur mostly on low-energy photons and increases as the material's atomic number decreases. On the other hand, the Compton effect occurs independently from the photons' energy and is related to the density of the material.

Material differentiation can occur when exposing the material to two different energies and comparing the energy spectrum that leaves the patient's body after the Compton and the photoelectric effects occur; materials such as iodine will have a large difference between the two attenuations from the two energies, meanwhile, materials such as the bones will have a smaller difference due to their difference in their atomic numbers.

These attenuation values are then used to decompose the material using a three-material decomposition algorithm; two of the three materials should have low atomic

numbers and the third material should have a high atomic number, for example, fat (low atomic number), soft tissue (low atomic number), and iodine (high atomic number) could be used. The algorithm then decomposes the voxels based on these three materials into two low atomic number elements and one high atomic number element allowing the identification and quantification of a certain material (Fornaro *et al.*, 2011).

2.11 Material Decomposition Clinical Application

The use of multi-energy CT imaging and material decomposition has found its way into multiple clinical applications where the need to identify a certain material is required to enhance the image quality and the diagnostic ability of the image, mentioned here are examples of clinical applications that use material decomposition.

Since spectral CT scanners use multi-energy photons, virtual Mono-energetic Image (VMI) can be created at different energy levels, VMI improves soft tissue contrast and reduces artifacts that are caused by beam-hardening, which is a serious problem for poly-energetic images.

Another application for material decomposition in spectral CT is bone removal in CT angiography since material decomposition allows the differentiation between the bones and other high-density materials, such as the iodinated contrast material. The removal of the signal coming from the bones will allow the creation of angiographic CT images where the iodinated vessels are clearly visualized without the bone obstructing the view. Similarly hard atherosclerotic plaques as well as calcium can also be identified and removed to better visualize the lumen of the blood vessels and the bone marrow respectively.

Spectral CT has many other clinical applications such as allowing color enhancement of areas filled with contrast creating perfused blood images, also called blood pool imaging, which can be done due to the scanner's ability to differentiate and identify iodinated contrast media. It has also the ability to discriminate between uric acid and non-uric acid stones by using material decomposition, and to differentiate between uric acid from calcium, as well as detecting silicon leaks from breast implants.

Another application for spectral CT using material decomposition is the creation of VNC images by detecting and subtracting the iodinated contrast material's voxels from the enhanced image, this way an additional acquisition is taken without exposing the patient to extra radiation (McCollough *et al.*, 2015).

2.12 Virtual Non-Contrast Images

Spectral CT scanners use material decomposition to differentiate materials with similar densities from each other such as bones, calcium plaques, and iodinated contrast material. Iodinated contrast material can be identified and removed from the enhanced scan to create a VNC image; that is an image without contrast material enhancement.

VNC images can be taken from any phase of contrast-enhanced scans whether from the arterial phase, the venous phase, or even the delay phase, after identifying the iodinated contrast material voxels, an iodine map can be created from any of these phases and then subtracted from the original enhanced image to create a VNC image without the need to scan the patient an extra scan and exposing them to additional radiation dose (Sauter *et al.*, 2018).

2.13 Previous Studies

Similar studies have been conducted to test the feasibility of using VNC images instead of TNC images since the emergence of spectral imaging and the creation of iodine mapping. Toepker *et al.*, (2012) conducted a study where 16 phantoms containing water and contrast materials with different percentages and different attenuation numbers (from 0 to 1400HU) were scanned on a single-energy CT protocol and a dual-energy CT protocol to create VNC images, the VNC and TNC images were then compared by creating a Region Of Interest (ROI) in the middle of the phantom and calculating the Mean Attenuation (MA) and the Standard Deviation (SD).

After conducting the phantom study, they made a clinical study where they brought 86 patients who underwent abdominal CT scans that consisted of a single-energy abdomen scan without contrast and a dual-energy abdomen scan with contrast where the contrast-enhanced scans for 43 patients were in the arterial phase and for the other 43 patients it was

in the venous phase, VNC images were created from the contrast-enhanced scans which means no comparison between the arterial and venous phases VNC images were made for the same patient, VNC images were then compared with the TNC images by placing ROIs in different points in the scan.

The results for the phantom study showed that the MA for all the VNC images was 5.3 ± 18.4 HU, and for the clinical study the MA for TNC images was 22.0 ± 49.9 HU, and for the TNC images, it was 25.6 ± 49.4 HU, which means the mean difference was only -3.6 ± 8.3 HU. The results concluded that VNC image attenuation numbers are close enough to the TNC attenuation numbers to be used in clinical scanning without reducing the diagnosis ability of the image.

To study the use of VNC images in specific medical cases, Sommer *et al.,* (2012) tested whether VNC images can replace TNC images if iodine removal was applied to contrast-enhanced acquisition during cholangiography where the contrast material is administrated intracellular, the study was done on 15 potential liver donors before liver transplantation, each patient was imaged in two phases, the first was without the injection of contrast media and using conventional imaging with one radiation source, and the second phase was a cholangiography exam after intravenous injection of contrast media using dual-energy spectral scanning.

VNC images were then created from the enhanced scan and compared to the TNC images in terms of subjective image quality, Contrast-to-Noise Ratio (CNR), SNR, and CT number accuracy. Even though the attenuation number differs significantly in the bile duct, gallbladder, kidney, and spleen between VNC images and TNC images, the researcher concluded that the difference does not have significant clinical relevance, and since the subjective image quality for VNC was equal to the TNC, the CNR was higher for the VNC, and the patient dose was reduced when VNC images were used, the study concluded that VNC images were an effective replacement for TNC images in cholangiography.

According to Kaufmann *et al.,* (2013), when they conducted a study to compare the image quality and the attenuation values between VNC and TNC images acquired by tin-filter dual-source CT scanner, the images gave similar results. The study consisted of 63

patients who underwent abdominal CT with and without contrast media, the contrast-enhanced images were taken during the portal-venous phase and VNC images were driven from them, MA was calculated for both images, and image quality was taken objectively by measuring image noise and edge sharpness.

The results showed that the mean of the attenuation values was close in most areas between the two images (except in the spleen and fat), and while image noise was higher in TNC images there was no significant difference in edge sharpness between the VNC and TNC.

A research made by Yoo *et al.*, (2013) have suggested the use of VNC images in place of TNC images in assessing mediastinal lymph nodes, 45 patients with 112 mediastinal nodes were enrolled in this study and after acquiring the TNC images and the VNC images from the contrast-enhanced images that were taken 40 seconds after contrast injection, the images were analyzed objectively using the CT number, and subjectively using visual-scoring in relation to the aorta, after that the data was further analyzed for comparison.

The results for the CT attenuation number showed moderate agreement with the MA difference being 7.8 ± 7.6 HU, while the visual score showed a fair agreement. This concluded that using VNC images in the assessment of mediastinal lymph nodes can be helpful but it doesn't rise to the level of replacing TNC images.

Other studies showed the feasibility of using VNC images in place of TNC images without comparing the origin of the VNC image, whether it was taken from contrast-enhanced arterial-phase CT or the venous phase.

When Tian *et al.*, (2015) conducted a study to evaluate VNC images in assessing hepatic metastases, they retrospectively collected 40 hepatic metastases patients' CT scans that included a non-enhanced scan as well as a tri-phasic contrast-enhanced scan in the arterial, venous, and equilibrium phases, VNC images were taken from the three phases to compare the image quality and the CNR between the three VNC images and the TNC images.

While this study didn't include comparing the attenuation numbers, it did show that the VNC images taken from the arterial phase and venous phase are similar in image quality

to that of the TNC images and that VNC images taken from the equilibrium phase have worse quality than the three mentioned before. This study was only limited to hepatic metastasis patients and it has another shortcoming in that it didn't include a comparison of the attenuation numbers between the three VNC image types and the TNC image.

To show the difference and compare the VNC images obtained from different phases of contrast-enhanced CT Ananthakrishnan *et al.*, (2017) tested 84 pairs of unenhanced and enhanced CT at different phases (25 arterial, 39 portal venous, and 20 uro-graphic), VNC images were obtained from all contrast-enhanced scans and ROIs were placed at six different sites in the abdomen, then the MA was calculated to check the difference between VNC and TNC Images. The results showed that there was no significant difference in the MA between phases and that 92.6% of the VNC images had an MA of less than 15 HU.

The main problem with this study was that the CT scans were collected from multiple institutions and the parameters for the imaging differed per institution. The type, timing, and dosage of the contrast media injected were not standardized, as well as the scan length, reference mAs, pitch, and gantry rotation time. Not standardizing the protocol parameter can affect the study's results.

Since then, multiple similar studies in the literature have searched the feasibility of using VNC images and how similar the image’s results will be in comparison with TNC images in different situations, but these studies limited their search to studying VNC images driven from one phase only. For example, Slebocki *et al.*, (2017) tested the use of VNC images in incidental findings during abdominal CT scans, and their study consisted of VNC images driven from the arterial phase only.

Additionally, Si-Mohamed *et al.*, (2019) conducted a study that consisted of a phantom study and a clinical study to assess VNC images in diagnosing intra-mural hematoma in place of TNC images to help in effective dose reduction, the clinical study also consisted of arterial-driven VNC images only, and in both the clinical and the phantom study, the CNR and the subjective image diagnosis confidence were the only variables collected and compared, without comparing the attenuation values of the images.

In another research, Jamali *et al.*, (2019) studied the potential dose reduction by using VNC images driven from the portal phase in abdominal or thoracoabdominal CT instead of TNC images. Similarly, Javadi *et al.*, (2020) showed the potential of using VNC images driven from the late arterial phase in assessing pancreatic cancer. All these studies gave similar results in that VNC images gave good agreement with TNC images in terms of attenuation numbers in most places and components of the body, and thus, can help utilize the use of contrast-enhanced images and discard the need for TNC acquisition to reduce the effective dose and scan time for the patient.

The difference in VNC images derived from different phases of the enhanced scan had been studied as well, but in most cases, it was limited to a specific organ or a certain disease. For instance, Lin *et al.*, (2018) wanted to compare renal parenchyma in VNC images in multiple phases scan in comparison with TNC images, three phases in contrast-enhanced renal imaging have been used to create three different types of VNC images, the cortico-medullary phase, the nephrographic phase, and the excretory phase.

After acquiring the three phases, a VNC image was derived from each phase and the attenuation numbers, as well as the image noise, were collected and compared. The results showed that the nephrographic phase produces a VNC image that is more similar to the TNC images in the renal parenchyma than the other phases.

Another study made by Sauter *et al.*, (2018) studied the difference between VNC images taken from two different phases, the arterial and the portal-venous phase. The study calculated the attenuation number in seven ROIs placed in different organs at the same location in each patient's scan.

And according to the results of this study, the VNC images taken from the arterial phase and the VNC images taken from the portal-venous phase were shown to be similar in the CT numbers, and that both can be used as an alternative for TNC images. A shortcoming for the study, that it didn't show which phase gave a VNC image more similar to the TNC image, and the focus in this study was on the CT number alone without including the image noise or the SNR.

According to a study conducted by Lehti *et al.*, (2019), the results have concluded that the VNC images based on the venous phase of the contrast-enhanced scan are more similar in attenuation number, image noise, and image quality to the TNC images than those based on the arterial phase, their study was only limited on endovascular aneurysm repair patients since these patients require life-long CT scan follow up after the repair and thus, are exposed to significant doses of radiation.

On the other hand, Laukamp *et al.*, (2020) found that the difference between VNC images that are based on the arterial phase and those based on the venous phase is negligible and both images can be used in place of TNC images. This study was made to evaluate VNC images only in the liver parenchyma and vessels, and it took into account both quantitative analyses such as CT number and image noise, and a visual analysis which was performed by two trained radiologists that rated the images' quality and its diagnosis ability on a 5-point Likert scale.

A recent study was conducted by Lee *et al.*, (2023) to assess the difference between TNC images and VNC images taken from multiple phases of contrast enhancement in the liver parenchyma, the scanning was done using two types of spectral scanners, a twin-beam single-source CT scanner, and a dual-source dual-energy CT scanner, the VNC images were derived from the arterial phase, the portal phase, and the delay phase.

When comparing the attenuation values between the TNC image and the VNC images the results showed a significant difference in the attenuation values, and concluded that not any of the VNC images types from neither the spectral scanners were sufficient to replace the TNC image, unlike the other studies' results that showed agreement in the attenuation values between the VNC images and TNC images.

Chapter Three: Methodology

3.1 Introduction

This segment discusses the design used to conduct this study, the patient population and the sample that was included in the study, the inclusion and exclusion criteria for the sample, and the ethical considerations about the study data. It will also explain the imaging parameters, the data collection method, and the statistical analysis that was done to reach the desired results.

3.2 Study Design

The current study is a quantitative observational cross-sectional study conducted at AL-Rahma clinic in Nablus/ Palestine. The study aims to compare VNC images driven from the arterial phase and the venous phase of an enhanced scan with TNC images for the abdomen. The images needed for the study were collected retrospectively from the clinic's data set after obtaining consent from the clinic, as the patients were all previously scanned for a multiphasic CT exam of the abdomen for various medical indications, the exam included an unenhanced scan, an arterial phase, and a venous phase, the imaging was all done using the clinic’s protocol for imaging a multiphasic abdomen CT scan.

3.3 Study Population

This study included 141 patients (79 female and 62 male, the range of age was between 13 and 89 years, with a mean age of 43 years) who underwent multiphasic abdominal CT scans with and without contrast material intake, their images were collected retrospectively and enrolled in the study. The patients were imaged between July 2022, when the spectral CT scanner was first installed, and October 2024. The patients were requested to undergo the multiphasic abdominal CT scan for various clinical indications such as

abdominal trauma, abdominal mass, aortic aneurysm, liver problems, kidney problems, or infections.

Before the exam, all the patients were checked for a history of allergic reaction to iodine or contrast media as well as underwent creatinine clearance blood test and made sure that the creatinine level was within the normal range (0.7 to 1.3 for males and 0.6 to 1.1 for females) so that the contrast material could be filtered from the body, the patients have also been instructed to fast for at least eight hours before the examination, and if the patient was diabetic that take metformin as a medication, then the patient is asked to withhold the medicine for 48 hours after the contrast intake during the exam.

3.4 Inclusion and Exclusion Criteria

The inclusion criteria for the sample were to include all the patients who underwent a multi-phasic abdominal CT scan on a spectral CT scanner using the imaging parameters that are used in imaging multiphasic abdominal scans, and that the patient had to undergo all the three phases that are used in the study, which are the non-enhanced phase, the arterial phase, and the venous phase scans and that included the abdominal area. The study included a number of patients who underwent CT scans for multiple regions but made sure that it included the abdominal area in the scan, such as a chest-abdomen scan, neck-chest-abdomen-pelvis scan, or a full body scan.

The study also included patients who were scanned multiphasic scans that included more phases than the ones needed for the study, such as scans that included one or more delayed phases to visualize the contrast location in the abdomen after a certain period of time. The study excluded any patient who didn't undergo one or two of the phases needed for the study, and also excluded any scans that did not cover the whole abdominal area as well as images that contained artifact in them that made it harder to collect the data needed for the study. The inclusion and exclusion criteria that were implemented in this study can be seen in (Table 3.1).

Table 3.1: The Inclusion and Exclusion Criteria for the Study

Inclusion criteria	Exclusion criteria
Undergoing unenhanced, arterial, and venous phases	Missing a phase from the scan
Including the abdominal area in the scan	Did not include the full abdomen
Scanned using abdominal multi-phasic scan parameters	Having artifact in the image

3.5 Ethical Consideration

The Institutional Review Board (IRB), which is associated with the Arab American University of Palestine (AAUP), has approved of the study and the method used to conduct this study (see appendix A), the study has also received approval from AAUP (see appendix B). Since the data was collected retrospectively, it wasn't possible to obtain consent from the participants themselves, and consent was only obtained from the clinic, though the clinic was assured that all the patient data collected for the study was used for research purposes only and that the data didn't include any sensitive personal information such as name, address, or phone number.

3.6 CT Parameters

All 141 patients were examined using the same abdomen protocol, which is the standard protocol that had been used in the clinic for imaging patients with orders for an abdominal CT scan with and without contrast. The images were taken on Philips's dual detector layer spectral CT scanner (Royal Philips, the Philips spectral CT 7500, Netherlands).

The scanner has a 512 slices dual-layer detector that receives low-energy photons in the first layer creating low-energy image, and high-energy photons in the second layer creating high-energy image, the two images are then added together to create spectral images

in addition to the conventional image for all scans without the need to pre-select the parameters to create the spectral image.

The imaging for each patient was done with the patient lying down supine on the CT scanner's table; the patient's arms were elevated above the head and the patient was scanned, during breath-hold, in craniocaudal direction from above the diaphragm to below the symphysis pubis to include the whole abdominal area, the scan started with the diaphragm to ensure that in case the patients was not capable of holding their breath, the diaphragm movement will not affect the image.

First, the scout view, or the scanogram, was taken in a frontal anterior-posterior projection and used to determine the Field Of View (FOV) and the length of the scan on each patient, it is also used to make sure that the patient is centered and positioned correctly, as well as to allow the scanner's AEC system to calculate the correct dose to use while scanning the patient, following the scout view, the non-enhanced scan of the abdomen was taken before injecting the patient with the contrast media for the arterial and the venous phases.

The volume dose of the contrast media used (Omnipaque 350 mg I/ml; GE Healthcare) was calculated for each patient based on their weight, with one ml of contrast media for each kilogram of the patient's weight, before contrast media injection, 10ml of normal saline is pushed into the patient, and after the contrast media injection, it is followed by injecting a 50ml normal saline chaser. Both the contrast media and the normal saline, before and after the contrast injection, were injected at a 3ml/s flow rate.

After the patient was injected with the contrast material and the saline chaser using a dual automated injector, both the arterial phase and venous phase were taken without using bolus tracking or test bolus techniques. The arterial phase was timed to be taken 30 seconds after contrast injection, then the venous phase to be taken 75 seconds after injection. For patients who underwent scans that covered more than the abdominal area, such as the chest-abdomen scan, the timing of the image acquisition after contrast injection was adjusted so that the abdomen scan would be taken when the contrast media passes the abdomen after 30s for the arterial phase and 75s for the venous phase.

The three acquisitions were taken using a tube potential of 120 kV and AEC was used to determine the needed mAs for each area based on its thickness on the X-Y axis and on the Z-axis from the measurements that were made during the imaging of the scout view, but the reference mAs that was used in the TNC image 78 mAs and for the arterial and venous phase it was 87 mAs. The rest of the parameters that were used for imaging the arterial phase, venous phase, and TNC images were similar between the three acquisitions and are listed below, as shown in Table (3.2). The arterial and venous phases were then reconstructed to produce a VNC image of each one of them.

The TNC images, the arterial phase images, and the venous phase images were then reconstructed using Philips' iDose^4 reconstruction algorithm with a 2.00 mm reconstructed slice thickness. And after opening the spectral data of the image, the VNC images were then created by automatic generation, from both the arterial phase and the venous phases for each patient.

Table 3.2: CT Scanning and Reconstruction Parameters Used for the TNC, Arterial Phase, and Venous Phase Images.

Parameters	TNC	Arterial phase	Venous phase
Tube potential, kV	120	120	120
Reference mAs	78	87	87
Pitch	1.386	1.386	1.386
Rotation time, s	0.27	0.27	0.27
FOV, mm	350	350	350
Matrix	512x512	512x512	512x512
Reconstructed slice thickness, mm	2	2	2
Reconstruction algorithm	iDose4	iDose4	iDose4

3.7 Image Quality Analysis

To analyze the image quality of the three scans a circular ROI was placed at five different places to test the attenuation values difference in different types of tissue within each acquisition; this was done using IntelliSpace Portal (ISP) workstation which is the standard workstation used in AL-Rahma clinic.

The first ROI was placed within the lumen of the aorta at the level of the diaphragm, the second was placed within the lumen of the aorta at the level of the renal arteries, the third was placed within the right lobe of the liver, the forth was placed within the retroperitoneal fat, and the fifth was placed within the psoas muscle. The size of the ROIs was different between the patients but consisted between the three acquisitions for the same patient. The placements of the five ROIs in the three acquisitions can be seen in figure (3.1-3.5).

While placing the ROIs within each scan for each patient, it was made sure to place each ROI at the same area between different scans for the same patient, and that the ROIs have the same size; this was done by placing the three acquisitions side by side to make sure they're on the same level on the Z-axis with the help of the coronal view, then after placing the first ROI on the TNC image the ROI was copied and pasted on the VNC-A image and then the VNC-V image. The placement of the ROIs was done while avoiding any calcifications plaques and stent materials, especially for the first two ROIs since they are placed within the lumen of the aorta.

From each ROI the MA and the SD were collected to compare the CT numbers in HU and the image noise, which is represented by the SD of the ROI, between the three acquisitions (see appendix C), and to compare the image quality, the SNR was also calculated for each ROI using the following formula, and compared between the images:

$$SNR = mean\ CT\ number/SD \qquad (2)$$

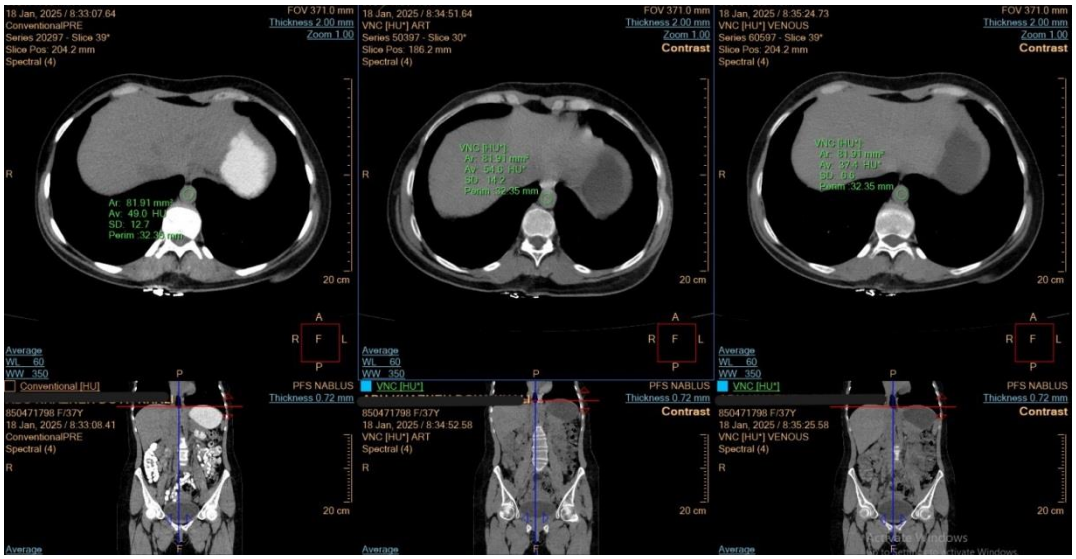

Figure 3.1: ROI (1) Placement within the Aorta at the Level of the Diaphragm in the TNC, VNC-A, and VNC-V Images.

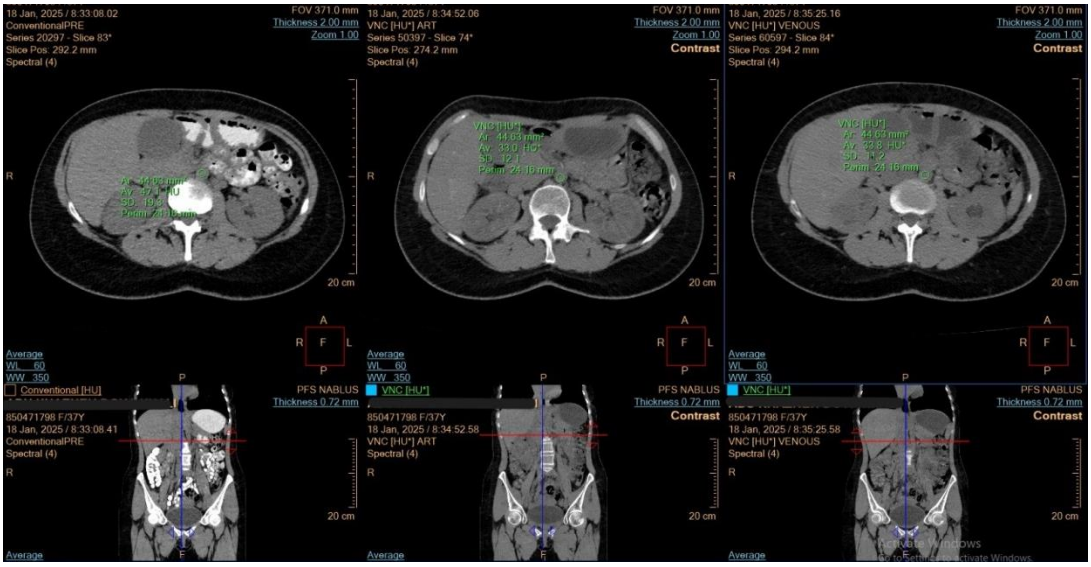

Figure 3.2: ROI (2) Placement within the Aorta at the Level of the Kidney's Arteries in the TNC, VNC-A, and VNC-V Images.

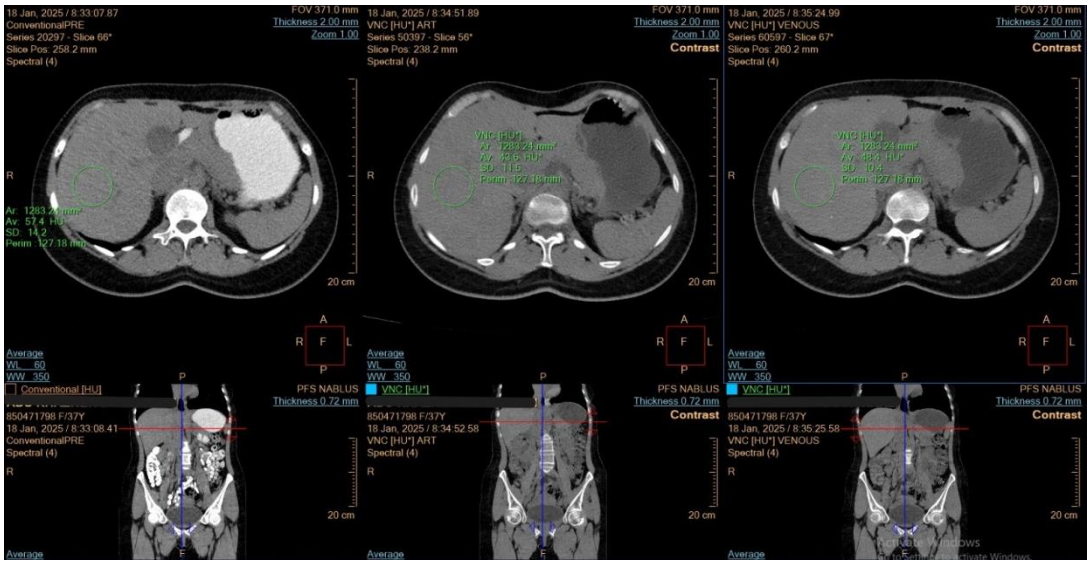

Figure 3.3: ROI (3) Placement within the Right Lobe of the Liver in the TNC, VNC-A, and VNC-V Images.

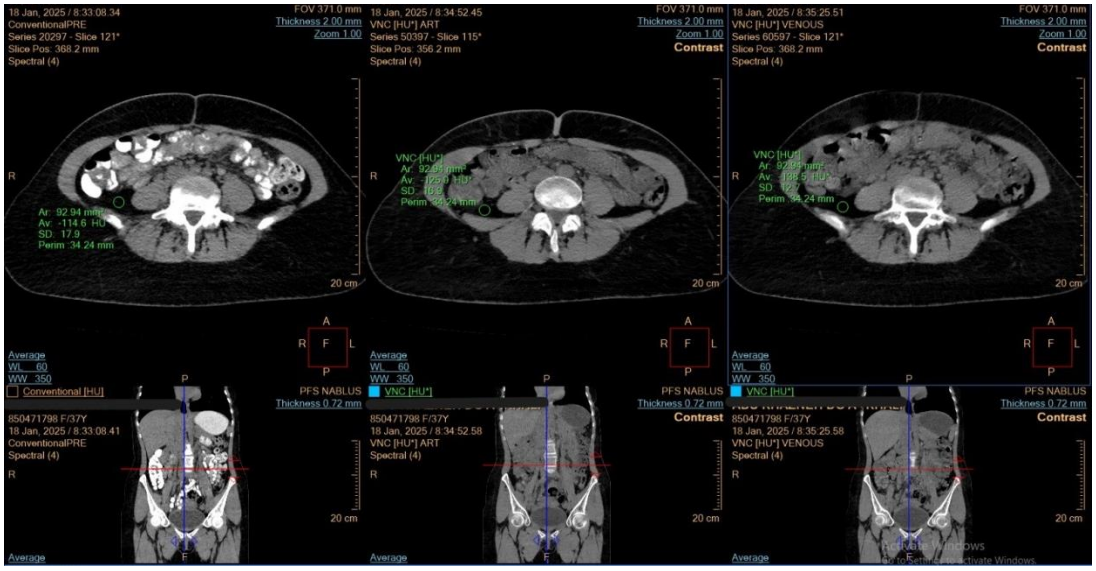

Figure 3.4: ROI (4) Placement within the Retroperitoneal Fat in the TNC, VNC-A, and VNC-V Images.

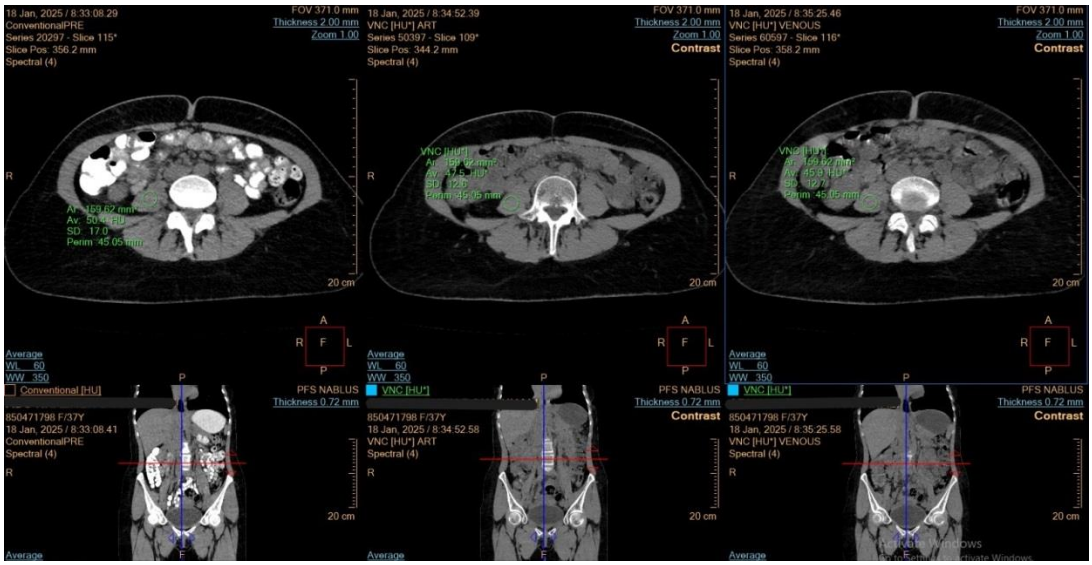

Figure 3.5: ROI (5) Placement within the Psoas Muscle in the TNC, VNC-A, and VNC-V Images.

3.8 Radiation Dose

Since the study was conducted to find a way to reduce the patient's dose, the total DLP for each patient was collected in order to calculate the amount of radiation and the effective dose that would be reduced if either of the VNC images were able to replace the TNC image.

Unfortunately, the only available dose reference type was the total DLP, which cannot be used for calculations, and not the DLP for each singular acquisition, and given the fact that some patients underwent different scan types with different scan lengths, and not just the standard abdominal scan, the DLP numbers had a wide range and no analysis nor any calculations took place to find out how much radiation will be reduced from the patient dose if the VNC images were able to replace the TNC images for abdominal scans.

3.9 Statistical Analysis

All the statistical analysis for this study and the creation of the scatter plots were done using the IBM Statistical Package for Social Sciences (SPSS) statistical software program version 25.0. To describe the distribution within the data, the mean and the median were used to measure the center, additionally; the maximum value and the minimum value were found.

To compare the CT number between the TNC, VNC-A, and VNC-V in terms of the MA and the SD, which is counted as the noise, the Mann-Whitney U test was used across all ROIs, which is a nonparametric test that is used to test the null hypothesis in the study by comparing two independent groups, and given the fact that the data is not normally distributed, the Mann-Whitney U test was the most suitable to use.

To test the VNC-A images and VNC-V images assessing similarity to TNC images Wilcoxon Signed-Rank test was used: this test is used when comparing two related samples to assess whether the mean ranks for the population differ significantly or not. The level of significance for all of the relations was set to P-value < 0.05.

Chapter Four: Results

4.1 Sample Characteristics

The sample consists of 141 participants, with 62 males and 79 females. The average age for males is 40 years, while the average age for females is 45 years. This indicates that, on average, females in this sample are slightly older than males. The overall average age among all participants is 43 years. The distribution of the sample can be seen in Table (4.1).

Table 4.1: Distribution of the Study Sample by Age and Gender

Variables		**Age**				
		N	Mean	Minimum	Maximum	Median
Gender	Male	62	40	13	86	39
	Female	79	45	13	89	43
Total		**141**	**43**	**13**	**89**	**42**

Where N is the number of the sample size.

4.2 Descriptive Statistics

The descriptive statistics for TNC, VNC-A, and VNC-V images across five ROIs, focusing on the MA and the SD of the attenuation values in the images are summarized in Table (4.2).

Table 4.2: Summary Statistics, TNC, VNC-A, and VNC-V Images across ROIs

Variables			Mean	Median	Std. Deviation	Minimum	Maximum
TNC	Aorta (Diaphragm)	MA	44.391	44.30	8.11	25.80	70.10
		SD	12.630	11.80	3.87	5.50	26.50
	Aorta (Renal)	MA	46.361	46.20	4.29	33.60	59.30
		SD	16.679	15.90	3.63	8.70	26.60
	Liver	MA	55.814	59.80	11.83	1.50	71.90
		SD	15.041	15.10	2.88	3.90	23.90
	Subcutaneous Fat	MA	-108.926	-109.70	8.09	-133.50	-67.20
		SD	16.860	17.10	3.63	5.80	29.40
	Psoas Muscles	MA	54.963	55.50	5.96	39.20	71.40
		SD	19.265	19.30	4.73	9.50	31.60
VNC-A	Aorta (Diaphragm)	MA	42.487	41.50	11.43	16.60	95.20
		SD	10.453	10.00	3.63	4.30	25.80
	Aorta (Renal)	MA	39.865	40.40	6.46	22.60	57.50
		SD	13.601	13.30	3.27	6.90	25.50
	Liver	MA	44.965	47.60	9.50	1.30	60.10
		SD	11.018	10.60	2.38	7.00	20.90
	Subcutaneous Fat	MA	-110.645	-112.80	9.36	-127.70	-56.40
		SD	13.503	13.10	4.24	7.00	47.70
	Psoas Muscles	MA	42.742	43.40	4.73	23.60	52.30
		SD	14.319	13.40	9.60	5.80	119.00
VNC-V	Aorta (Diaphragm)	MA	35.909	35.40	9.05	16.70	71.00
		SD	10.342	9.70	3.47	3.50	22.70
	Aorta (Renal)	MA	34.657	35.10	5.36	20.50	52.10
		SD	13.755	13.90	3.72	7.50	31.10
	Liver	MA	45.595	48.50	9.56	4.50	61.00
		SD	11.460	11.10	2.30	6.70	18.20
	Subcutaneous Fat	MA	-108.585	-110.50	10.04	-124.20	-55.10
		SD	14.406	13.50	7.45	7.30	92.00
	Psoas Muscles	MA	43.510	43.60	4.37	29.20	57.10
		SD	13.705	12.90	3.63	7.00	26.20

Where MA is the Mean attenuation and SD is the Standard Deviation.

Keeping in mind that the placements of the five ROIs are identified as follows:

ROI (1) is within the aorta at the level diaphragm
ROI (2) is within the aorta at the level of the renal arteries
ROI (3) is within the right lobe of the liver
ROI (4) is within the retroperitoneal fat
ROI (5) is within the psoas muscle

TNC shows higher mean values than both VNC-A and VNC-V in ROI (1), ROI (2), ROI (3), and ROI (5). In ROI (1), TNC has a mean MA of 44.39, compared to 42.49 for VNC-A and 35.91 for VNC-V.

The inconsistency is found in ROI (2), where TNC's mean MA (46.36) exceeds VNC-A (39.87) and VNC-V (34.66) by substantial margins. In ROI (4) all three methods show similar mean values, with TNC at -108.93, VNC-A at -110.65, and VNC-V at -108.59, reflecting comparable trends.

For SD, which represents the image noise in the ROIs, TNC also demonstrates higher variability than VNC-A and VNC-V in most ROIs. In ROI (1), TNC's SD mean is 12.63 compared to 10.45 for VNC-A and 10.34 for VNC-V. The highest variability was in ROI (5), where TNC's SD mean is 19.27, higher than both VNC-A (14.32) and VNC-V (13.71).

To clearly observe the relation of the MA between TNC images, VNC-A images, and VNC-V images across the five ROIs, five scatter plots which can be seen in figure (5.1-5.5) have been created which show that TNC images have higher mean MA values than both VNC-A and VNC-V across all ROIs.

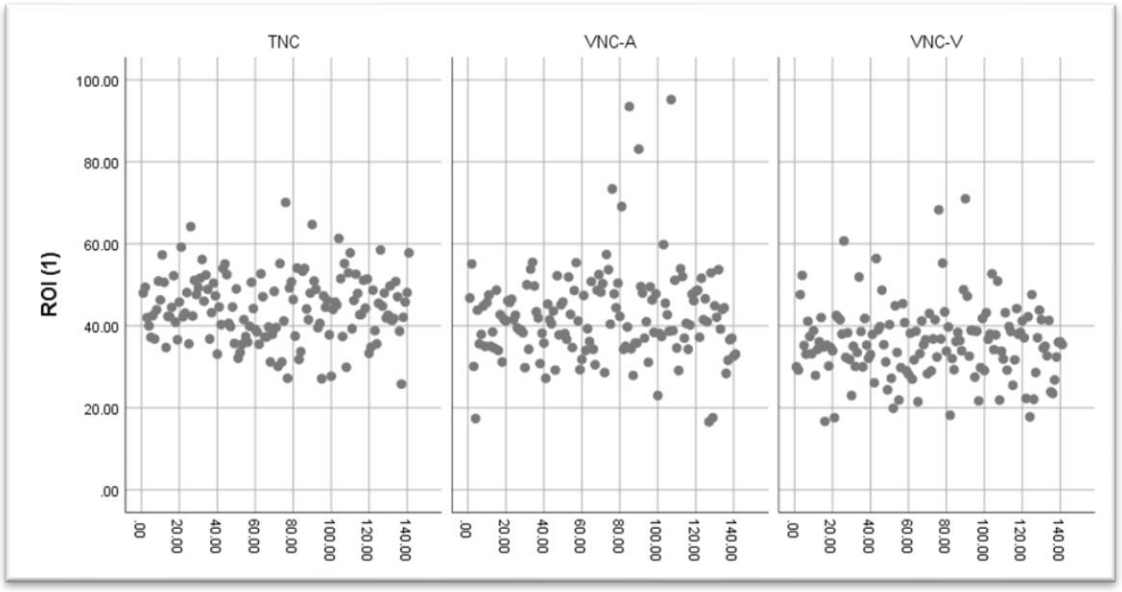

Figure 4.1: Scatter Plot Representing the MA at TNC, VNC-A, and VNC-V at ROI (1)

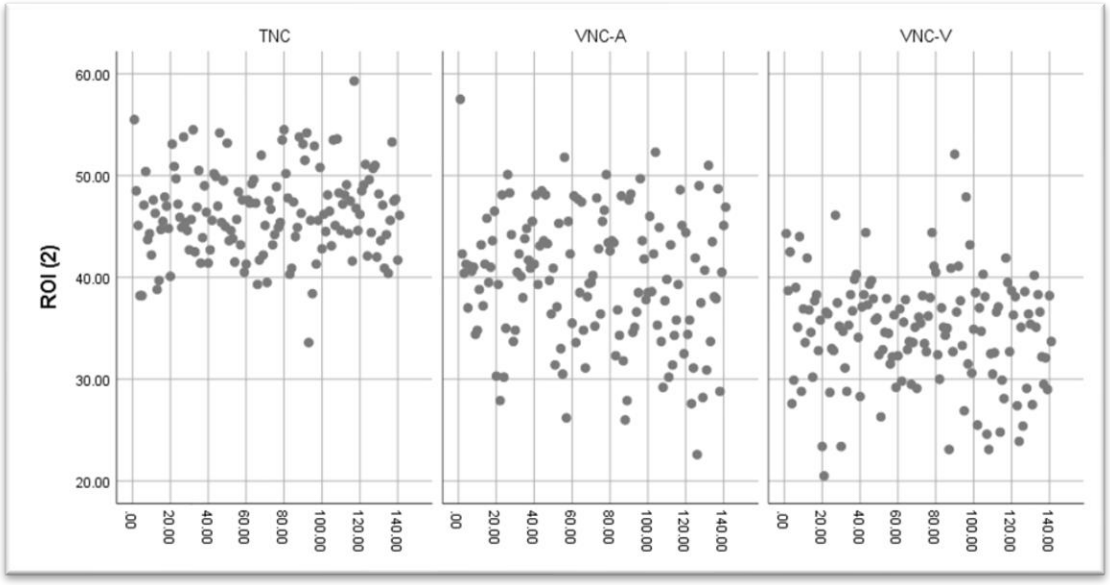

Figure 4.2: Scatter Plot Representing the MA at TNC, VNC-A, and VNC-V at ROI (2)

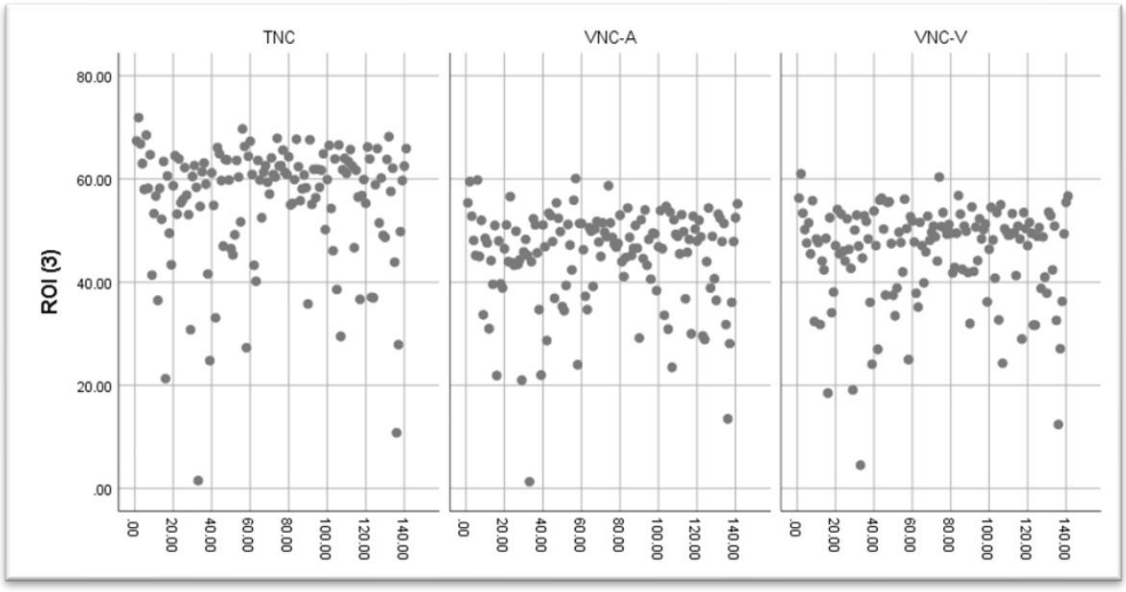

Figure 4.3: Scatter Plot Representing the MA at TNC, VNC-A, and VNC-V at ROI (3)

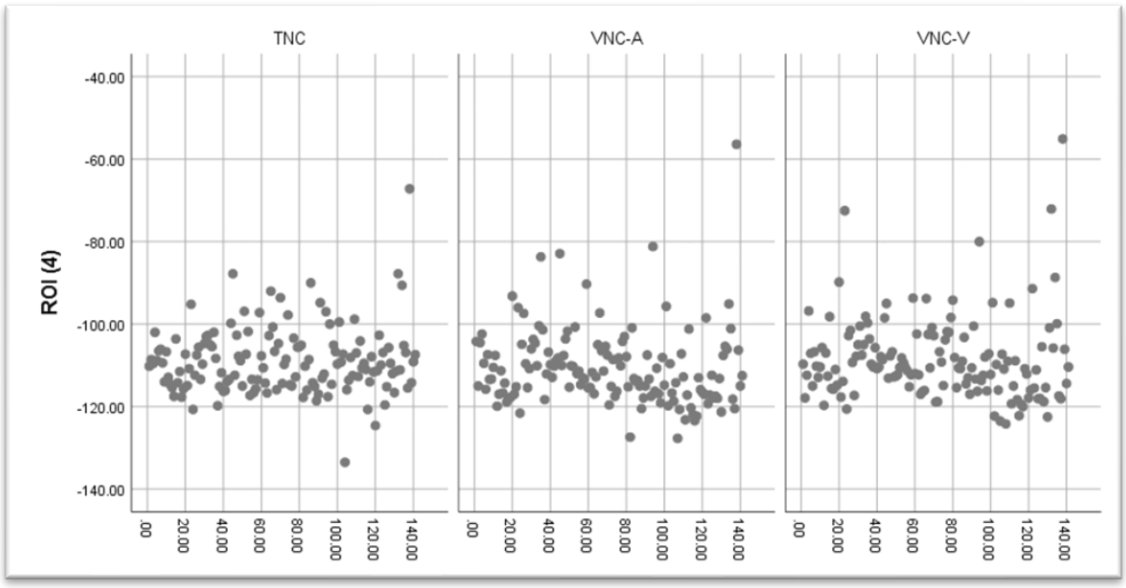

Figure 4.4: Scatter Plot Representing the MA at TNC, VNC-A, and VNC-V at ROI (4)

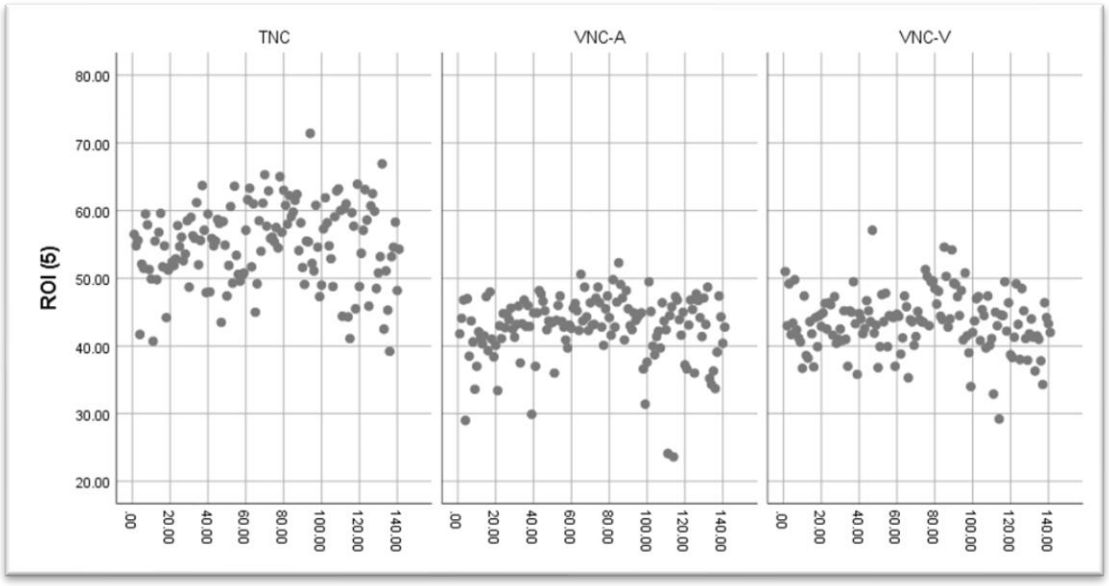

Figure 4.5: Scatter Plot Representing the MA at TNC, VNC-A, and VNC-V at ROI (5)

4.3 Inferential Statistics

The Mann-Whitney U test was performed to compare CT numbers accuracy and image noise between TNC images, VNC-V images, and VNC-A images across the ROIs for the metrics of MA and SD. Wilcoxon Signed-Rank test was used to assess the similarity to TNC.

The results showed that there were statistically significant differences between TNC images and VNC-A images in all ROIs for both MA and SD. TNC had higher mean ranks than VNC-A.

In ROI (1), for MA, the significance value was 0.012, and the mean rank of TNC was 153.67 compared to 129.33 for VNC-A. For SD, the significance value was 0.000, with a mean rank of TNC of 165.26 compared to 117.74 for VNC-A.

Table 4.3: Mann-Whitney U Test Results, comparing TNC and VNC-A across ROIs

Variables		Mean Rank	△ TNC-VNC-A	Sig.
ROI(1) MA	TNC	153.67	24.34	0.012
	VNC-A	129.33		
ROI(1) SD	TNC	165.26	47.52	0.000
	VNC-A	117.74		
ROI(2) MA	TNC	182.56	82.12	0.000
	VNC-A	100.44		
ROI(2) SD	TNC	175.04	67.08	0.000
	VNC-A	107.96		
ROI(3) MA	TNC	186.84	90.68	0.000
	VNC-A	96.16		
ROI(3) SD	TNC	194.35	105.70	0.000
	VNC-A	88.65		
ROI(4) MA	TNC	154.1	25.20	0.000
	VNC-A	128.9		
ROI(4) SD	TNC	181.21	79.42	0.000
	VNC-A	101.79		
ROI(5) MA	TNC	204.59	126.18	0.000
	VNC-A	78.41		
ROI(5) SD	TNC	186.9	90.80	0.000
	VNC-A	96.1		

In comparing TNC and VNC-V images, the largest mean difference was observed in ROI (2) for mean MA, where TNC was 130.23 ranks higher than VNC-V (p<0.001), followed by a difference of 98.01 ranks in ROI (3) for SD (p<0.001). The smallest difference was in ROI (4) for MA, with a rank difference of only 4.40 (p<0.001).

Table 4.4: Mann-Whitney U Test Results, comparing TNC and VNC-V across ROIs

Variables		Mean Rank	△ TNC-VNC-V	Sig.
ROI (1) MA	TNC	180.5922	78.18	0.000
	VNC-V	102.4078		
ROI (1) SD	TNC	166.1596	49.32	0.000
	VNC-V	116.8404		
ROI (2) MA	TNC	206.617	130.23	0.000
	VNC-V	76.38298		
ROI (2) SD	TNC	172.6418	62.28	0.000
	VNC-V	110.3582		
ROI (3) MA	TNC	185.5177	88.04	0.000
	VNC-V	97.48227		
ROI (3) SD	TNC	190.5035	98.01	0.000
	VNC-V	92.49645		
ROI (4) MA	TNC	143.6986	4.40	0.000
	VNC-V	139.3014		
ROI (4) SD	TNC	174.7624	66.52	0.000
	VNC-V	108.2376		
ROI (5) MA	TNC	202.5851	122.17	0.000
	VNC-V	80.41489		
ROI (5) SD	TNC	186.3582	89.72	0.000
	VNC-V	96.64184		

Table 4.5: Mann-Whitney U Test Results, comparing VNC-A and VNC-V across ROIs

Variables		Mean Rank	△VNC-V -VNC-A	Sig.
ROI(1) MA	VNC-A	169.00	-55.00	0.000
	VNC-V	114.00		
ROI(1) SD	VNC-A	142.84	-2.68	0.783
	VNC-V	140.16		
ROI(2) MA	VNC-A	174.37	-65.74	0.000
	VNC-V	108.63		
ROI(2) SD	VNC-A	140.54	1.92	0.844
	VNC-V	142.46		
ROI(3) MA	VNC-A	136.76	9.48	0.329
	VNC-V	146.24		
ROI(3) SD	VNC-A	132.09	18.82	0.053
	VNC-V	150.91		
ROI(4) MA	VNC-A	131.75	19.50	0.045
	VNC-V	151.25		
ROI(4) SD	VNC-A	135.68	11.64	0.230
	VNC-V	147.32		
ROI(5) MA	VNC-A	138.70	5.60	0.564
	VNC-V	144.30		
ROI(5) SD	VNC-A	140.27	2.46	0.801
	VNC-V	142.73		

In the differences in the mean ranks between VNC-A images and VNC-V images across the ROIs, we found that in ROI (1) and ROI (2) for MA, the VNC-A ranks were higher than the VNC-V ranks with a statistical significance of ($p<0.001$), also in ROI (4) for MA, the ranks for VNC-A were lower than VNC-V, while the other regions did not show statistically significant differences.

These non-significant results highlight the consistency between VNC-A and VNC-V across specific ROIs and measures, particularly for SD, where differences in mean ranks were small. This suggests that the two image types may provide similar mean attenuation values, and similar image noise, and have similar image quality and diagnostic ability in this context.

4.4 Research Questions and Hypotheses:

Main Hypothesis: VNC images based on the venous phase are more similar to the TNC images than the VNC images based on the arterial phase in terms of CT number accuracy.

Main question: Which VNC image is more similar to the TNC image in terms of CT number accuracy, VNC images based on the arterial phase or VNC images based on the venous phase?

The Wilcoxon Signed Ranks Test results reveal significant differences among VNC-A, VNC-V, and TNC metrics across various configurations. A general index for VNC-A, VNC-V, and TNC was calculated by averaging the values of the five ROI items for both MA and SD, as shown in Table (4.6).

Table 4.6: Wilcoxon Signed Ranks Test Results Comparing VNC-A, VNC-V and TNC

Variable		N	Mean Rank	Sum of Ranks	Sig.
VNCA_MA - TNC_MA	Negative Ranks	137	72.9781	9998	0.000
	Positive Ranks	4	3.25	13	
	Ties	0			
VNCV_MA - TNC_MA	Negative Ranks	140	71.5	10010	0.000
	Positive Ranks	1	1	1	
	Ties	0			
VNCV_MA - VNCA_MA	Negative Ranks	105	76.38571	8020.5	0.000
	Positive Ranks	36	55.29167	1990.5	
	Ties	0			
VNCA_SD - TNC_SD	Negative Ranks	138	71.04348	9804	0.000
	Positive Ranks	3	69	207	
	Ties	0			
VNCV_SD - TNC_SD	Negative Ranks	138	71.45652	9861	0.000
	Positive Ranks	3	50	150	
	Ties	0			
VNCV_SD - VNCA_SD	Negative Ranks	60	66.11667	3967	0.044
	Positive Ranks	86	74.7093	6425	
	Ties	3			

The results in Table (4.6) show that:

1. VNCA_MA - TNC_MA: Negative ranks (137) and significant difference (p=0.000) indicate that VNC-A differs significantly from TNC images in terms of the accuracy of the CT number.

2. VNCV_MA - TNC_MA: Negative ranks (140) and significant difference (p=0.000) also indicate that VNC-V differs significantly from TNC images.

However, the number of positive ranks is less (1 vs. 4), and the mean rank of negative ranks is smaller in VNC-V (72.9781 vs. 71.5).

3. VNCA_SD - TNC_SD and VNCV_SD - TNC_SD: Both arterial and venous phases show significant differences (p=0.000) in standard deviation compared to TNC, suggesting variability.

4. VNCV_SD - VNCA_SD: Significant (p=0.044) with positive ranks (86) and higher mean rank (74.7093). Suggests that VNC-V images are less variable and closer to TNC than VNC-A images in terms of standard deviation.

Conclusion:

VNC-A appears to be more similar to TNC than VNC-V based on ranks and differences.

Sub-question 1: Can VNC images derived from either the arterial phase or the venous phase replace TNC images in abdominal scans?

As shown in Table (4.6): we note that:

1. The consistent significant differences (p=0.000) for both VNCA_MA - TNC_MA and VNCV_MA - TNC_MA suggest that neither arterial phase-based VNC images nor venous phase-based VNC images are identical to TNC images.

2. While VNC-A images are closer in similarity to TNC than VNC-V, the differences remain statistically significant.

Conclusion:

Neither VNC-A images nor VNC-V images can fully replace TNC images in abdominal scans due to significant differences in the MA.

Sub-question 2: How different are the CT number readings from arterial VNC images and venous VNC images in comparison to the TNC images?

As shown in Table (4.6): we note that:

1. VNCA_MA - TNC_MA: A larger mean rank (72.9781) indicates smaller differences from TNC compared to VNC-V.

2. VNCV_MA - TNC_MA: Smaller mean rank (71.5) indicates bigger deviation from TNC than VNC-A.

3.VNCV_MA - VNCA_MA: Significant differences (p=0.000) show that venous and arterial VNC images differ in CT number accuracy, while positive ranks (36) and smaller mean rank (76.38571) indicate that VNC-A generally performs better than VNC-V.

Conclusion:

CT numbers from arterial VNC images are closer to TNC images compared to venous VNC images, as indicated by smaller rank differences and fewer positive ranks.

Sub-question 3: How different is the image quality between the arterial VNC images and venous VNC images in comparison to the TNC images?

Based on Table (4.7), the differences between VNC-A, VNC-V, and TNC images were assessed using the SNR after being calculated using the formula in equation (2).

The analysis reveals that VNC-A images have significantly lower SNR compared to TNC images (p=0.000). Similarly, VNC-V images also have significantly lower SNR compared to TNC images (p=0.000).

While VNC-A images show slightly better SNR performance than VNC-V images in comparison to the TNC images, both VNC image types remain significantly different from the TNC image.

Table 4.7: Wilcoxon Signed Ranks Test Results Comparing VNC-A_SNR, VNC-V_SNR and TNC_SNR

Variable		N	Mean Rank	Sum of Ranks	Sig.
VNCA_SNR - TNC_SNR	Negative Ranks	112	74.67	8363.00	0.000
	Positive Ranks	29	56.83	1648.00	
	Ties	0			
VNCV_SNR - TNC_SNR	Negative Ranks	130	74.65	9705.00	0.000
	Positive Ranks	11	27.82	306.00	
	Ties	0			
VNCV_SNR - VNCA_SNR	Negative Ranks	104	77.47	8057.00	0.000
	Positive Ranks	37	52.81	1954.00	
	Ties	0			

Conclusion:

Both VNC-A_SNR and VNC-V_SNR are significantly lower than TNC_SNR, indicating reduced image quality in terms of SNR for both VNC types compared to TNC.

Chapter Five: Discussion and Conclusion

5.1 Introduction

In this section, the results of the study will be discussed thoroughly, explaining the meaning, importance, and relevance of the results. The outcome of this study will be compared with the results from previous studies conducted around the same topic, and the differences between the studies' results will be highlighted.

This section will also highlight the conclusion that came out of this study, give a few recommendations based on the findings, explain the strength points and the limitations of the study, and recommend topics for future works and studies that will help find out more about the topic of the study.

5.2 Discussion

Decreasing the patient dose in CT is a topic with major importance that multiple studies have been conducted to find a way to accomplish to reduce the potential hazard of X-ray on the patient (Hara *et al.*, 2013), one of the ways that was suggested was to reduce the amount of acquisitions needed in a certain scan without decreasing the scan's diagnostic ability.

The current study has searched the feasibility of using VNC images driven from the arterial phase and the ones driven from the venous phase using spectral CT instead of TNC images in abdomen imaging, if VNC images from either phases were able to replace TNC images, one whole acquisition from multiphasic scans could be eliminated reducing by that the patient dose and the time spent in the scanning room.

Eliminating the need for TNC scans and reducing the patient dose shouldn't be done at the expense of the image quality and the diagnosis accuracy of the scan, since it may cause more harm than help to the patient and the medical team. For example, if the VNC image

had a higher noise level than the TNC image or if the image quality was degraded to the point where the patient's condition was misdiagnosed, it will cause harm to the patient and their treatment plan or it might even require requesting a repeated scan, and that will take longer time than needed and will expose the patient to more doses of radiation.

To create a VNC image, the enhanced pixels that are a representation of the iodinated contrast material are identified and subtracted from the original enhanced scan, whether it is from the arterial phase or the venous phase, to create an image without the contrast enhancement, any mistake that occur with the identification or the subtraction process will negatively affect the accuracy of the VNC image.

To make sure that only the iodinated pixels were removed and that they were removed accurately, in this study, the CT number in both types of VNC images and the TNC images is calculated and compared to make sure that the results are similar enough for the VNC images to replace the TNC images without degrading the accuracy of the attenuation values.

The accuracy of the CT numbers is critical and plays a major role in multiple clinical applications, such as in the quantitative measurements that calculate the change of the attenuation numbers from before and after contrast media enhancement, if the CT number was inaccurate in these measurements, whether it was before or after the contrast enhancement, it will affect the calculations and the decision-making process done by the radiologists (Zhang *et al.*, 2018).

Quantitative measurements are also done in other clinical applications such as when measuring adrenal and renal lesions, the composition of renal stones, cerebral venous thrombosis, abnormalities in the airway, measuring the extent of coronary atherosclerosis, and hepatic stones' measurements (Al-Hayek *et al.*, 2022).

The importance of the accuracy of CT numbers can also be seen in radiation therapy treatment planning and PET/CT imaging, the accuracy of CT numbers in these cases is extremely critical since the image data are used to outline the contour, shape, density of the internal organs, and the dose coverage, any inaccuracy in the CT number readings will affect the measurements of the treatment planning and will either expose more area than it should

to ionizing radiation, or not cover the whole targeted area (Zhang *et al.*, 2018; Al-Hayek *et al.*, 2022).

When comparing VNC images to TNC images, the CT number accuracy should be one of the most prioritized aspects of comparison, care should be taken to make sure that when subtracting the iodine voxels from the enhanced image to create the VNC image, no other material should be subtracted nor incomplete iodine subtraction would occur, that way accurate CT number in VNC images would be achieved.

In a conventional enhanced CT scan the HU range for trabecular bone, which is found at the end of long bones, is from 300 to 800 HU, while for the iodinated contrast material, the range is between 100 to 600 HU (Seeram and Sil, 2013), that means that the HU, which is based on the material's attenuation coefficient, alone is not enough to distinguish between the two materials.

In spectral CT, material decomposition and differentiation are achieved since imaging doesn't only depend on the material's attenuation coefficient, it depends as well on the response of the material to being exposed to the X-ray photons in multiple energy spectra, the photons will then leave the body holding information about the material composition based on its K-edge. Materials with high atomic numbers have high K-edge so the likelihood of the photoelectric effect occurring in them when exposed to photons is higher since the possibility of photoelectric effects increases when the atomic number increases.

The human body mostly consists of atoms with low atomic numbers such as hydrogen (1), carbon (6), and oxygen (8), but some atoms such as calcium (20) have a higher atomic number. When using iodinated contrast material during imaging the contrast provides a high photoelectric effect since the atomic number for iodine is (53), and so the difference in spectral behavior between iodine and the rest of the body is high on spectral images and can be used to detect and differentiate the iodine atoms (Johnson, 2012).

According to Lehti *et al.*, (2019) when they made a study to compare VNC images from the arterial and venous phases with TNC images for patients after endovascular aneurysm repair, the results showed that there was a significant difference in the attenuation values between the two types of VNC images and the TNC images in the ROIs placed at the

liver, subcutaneous fat, and muscle tissue, the difference was also seen between VNC-A images and TNC images at the two remaining ROIs in the aorta at the level of the diaphragm and at the level of the renal artery.

In this study, the ROIs were placed in the same areas as in the study made by Lehti *et al*., and while in their study the difference between VNC-V images and TNC images in the attenuation values was not significant at the lumen of the aorta, in our study there was a significant difference in the MA between both VNC images type and TNC images at all ROIs, making VNC images infeasible to replace TNC images without reducing the diagnostic ability of the image taken from accurate measurement of the CT numbers.

Although most previous studies stated that VNC images are capable of replacing TNC images for certain medical cases, these studies have also shown agreement with our study in the fact that there was still a difference in the attenuation values between the two images, for example, a study conducted to test the image quality in VNC images acquired by tin-filter enhanced dual-energy CT showed that in the spleen and fat, the HU tends to be significantly higher in the VNC images than in TNC images when the images are taken from the late arterial phase (Kaufmann *et al.*, 2013).

Another study has found differences in the attenuation values between VNC images taken from cortico-medullary phase and TNC images in the kidney's medulla, the VNC image had a lower attenuation numbers than the TNC image, the difference was also found in the renal cortex where the attenuation values for the VNC images driven from the nephrographic phase were higher than in the TNC images (Lin *et al.*, 2018), concluding that VNC images can differ significantly from TNC images in different types of tissue.

And according to Ananthakrishnan *et al.*, (2017), it was concluded that the VNC images taken from multiple different phases in abdominal scans have significant differences in the attenuation values from TNC images in the subcutaneous fat. Meanwhile, a study conducted by Jamali *et al.*, 2019 also resulted in fat having significantly higher attenuation values in VNC images compared to TNC images, and that concluded that if the studied organ during the CT exam contained mostly fat tissues, the VNC image would not be accurate to replace the TNC image.

There was also a study made in 2020 that studied CT scans of the liver, and it showed an inadequate iodine subtraction in the common hepatic artery when the VNC image was being driven from the arterial phase (Laukamp *et al.*, 2020).

According to Sommer *et al.*, (2012) in their search conducted about the feasibility of using VNC images taken from cholangiography scans that are done on potential liver donors instead of TNC images, have measured and compared the attenuation values, CNR, and the subjective image quality of the scan.

Since both the CNR and the subjective image quality were similar to the TNC or even better than the TNC, the study deemed VNC images as a feasible replacement for TNC images even though the study agreed with our results in the fact that the attenuation values in VNC images are significantly different from that in TNC images, in there study the difference was found in the bile duct, the gallbladder, the kidneys, and the spleen.

The results of this current study agree with the results from a recent study conducted in Korea, Lee *et al.*, (2023) studied 62 abdominal VNC images and TNC image pairs taken with two types of spectral CT scanners, which are the twin-beam dual-energy CT scanner and the dual-source dual-energy CT scanner, VNC images were reconstructed from the arterial phase, venous phase, and delayed phase, the ROIs were placed in 11 different places in the abdomen, and when the attenuation values were collected from the TNC image and the three VNC image types and compared, the results showed that there were significant differences in more than half of the regions in the abdomen.

The results concluding that, due to the difference in the attenuation values, none of the VNC images types were sufficient to replace the TNC image. This was the only study found in the literature that agreed with the results and the conclusion of the current study.

As shown from the results of this current study and the studies mentioned, iodine subtraction using spectral CT is still not optimum to the extent that VNC images can completely replace TNC images, meaning that spectral CT material decomposition and differentiation for iodinated contrast material is not completely accurate, and when creating VNC images the spectral scanner might misidentify other materials as iodine and subtract

them from the image, or might incorrectly not identify voxels containing iodinated contrast material as such and leave them in the image.

Incorrect quantification and decomposition of iodine in spectral CT have been studied and reported in previous studies, the reason for these miscalculations being the fact that the quantification of a material depends on certain assumptions, if these assumptions were incorrect, errors in the material's quantification will occur. These assumptions are based on the relationship between CT numbers, linear attenuation coefficient, and element density.

An understanding was driven from these reports that because of these assumptions, iodine-water material decomposition could never be completely accurate, and for material decomposition to occur without any errors only the materials that represent the basis for material decomposition should be inside the voxel without any other materials (Salyapongse and Szczykutowicz, 2024).

Keeping the image noise to a minimum and the SNR to a maximum is as critical to the diagnosis content of the image as the accuracy of the CT number (Abdulkareem *et al.*, 2023), different types of image noise such as random noise, statistical noise, electronic noise, and round-off errors, can have different appearances on the image based on the source of the noise (Diwakar and Kumar, 2018), but in most cases it is seen as unwanted artifact that compromise the subjective image quality and visibility and reduce the diagnostic value of the image.

It is known that image noise affects the contrast sensitivity of CT, and that is critical in an unenhanced scan since it will be more difficult to visualize low-contrast structures, given the fact that they are not enhanced with contrast material, with the presence of image noise. High SNR is therefore needed to achieve high diagnosis accuracy, and if the VNC images were to replace the TNC images, the image noise and SNR should be calculated and compared to make sure they are similar enough to not reduce the image quality and the diagnostic ability of the scan.

In the current study, the image noise was represented as the SD of the five ROIs that were placed in different places of the abdomen, and in all the ROIs the image noise in the

TNC images was significantly higher than the image noise in both the VNC-A images and the VNC-V images.

While not many studies that have been conducted to test the feasibility of using VNC images instead of TNC images had included image noise in the comparison point between the VNC images and TNC images, this study's results agreed with both Kaufmann *et al.*, (2013) results and Lin *et al.*, (2018) results in their studies regarding the feasibility of using the VNC images in place of the TNC images in the upper abdomen and in the kidneys respectively, where they found that the image noise in VNC images is significantly lower than in TNC images, yielding an increase in image quality for VNC images in terms of the image noise.

Other studies have found that the image noise in VNC images and TNC images is at a similar level and that there was not any significant differences between the two images, such as the study conducted by Lehti *et al.*, (2019) and the study conducted by Laukamp *et al.*, (2020) where the image noise at different segments of the liver was calculated, based on the SD of the ROIs, and compared to the TNC images from both the VNC-A and VNC-V images.

The SNR for the TNC, VNC-A, and VNC-V images was calculated using the formula in equation (2), as the equation suggested, the SNR and the image noise are inversely proportional, and if the mean attenuation values in our study were similar between the two VNC images types and the TNC images, then the SNR might be higher in the VNC images, since the image noise in the TNC images is higher, but because of the inconsistency of the attenuation numbers, the SNR turned out to be significantly higher in the TNC images, concluding a decrease in the image quality in the VNC images in term of the SNR.

The results for this study showed that the SNR was higher on the VNC images across all ROIs placed in different places in the abdomen, but when another study did their research regarding VNC images for the abdomen, the results, when comparing the SNR between the images, reported that the SNR was higher in the TNC images at the kidneys, subcutaneous fat, and perirenal fat, while the VNC images had a higher SNR at the liver, the spleen, and

the muscles, meaning the difference in SNR between images differ depending on the type of tissue that was imaged (Jamali *et al.*, 2019).

5.3 Conclusion

Spectral CT scanners have made it possible to generate images with high image quality, less radiation dose, and less contrast dose, the specialty of these scanners though, is their ability to decompose materials to identify and differentiate them from other materials, which can lead to the creation of multiple other spectral images with this technique such as VNC images. This study was conducted to test the feasibility of using VNC images driven from the arterial phase and the venous phase instead of TNC images to reduce the patient dose and to choose which VNC type is more similar to the TNC image so that it can be used to replace it without compromising the image quality and its diagnostic ability.

VNC images showed a significant difference in the MA from the TNC images, and a significant reduction in the SNR of the image, which means VNC images have different and inaccurate attenuation values compared to TNC images, as well as, that both types of VNC images have lower image quality based on the SNR of the image compared to the TNC image, concluding that neither VNC image type was similar enough to replace the TNC image without degrading the image quality and diagnosis ability.

5.4 Recommendations

From this study it was concluded that VNC images cannot replace TNC images, since they have a significant difference in terms of the attenuation values, using VNC images in medical cases that require accurate CT numbers, such as when measuring the uptake of the contrast material at a certain region or organ, will decrease the diagnosis ability of the scan and might cause misdiagnosis of the patient's condition, that is why VNC images are not recommended to use on these cases.

However, VNC images might be useful in some cases, for example, in cases where the institution imaging the patient excluded the unenhanced phase from the scan to reduce

the patient's dose, and after the scan the radiologist thought it would be helpful with the diagnosis to have an acquisition without contrast material, VNC images could be used, since the detector-based spectral CT scanner generates spectral data without the need to pre-select the parameters before the exam while keeping in mind the inaccuracy of the attenuation values in the image.

And to test the feasibility of using VNC images, more studies should be done to compare VNC images and TNC images in specific patients and types of diseases and in specific regions of the body and types of tissue, the results may suggest that VNC images are feasible to replace TNC images during these situations.

5.5 Strength of the Study

The strength of this study lies in the fact that this study falls directly into the practice of VNC images and their contribution to reduce the patient dose and testing the effect that contribution has over the diagnosis ability of the scan, the results of this study could be used directly in the practice of spectral imaging.

Unlike other studies that have tested the use of VNC images in certain organs or certain clinical cases, this study tested the way VNC images could be utilized in all patients without any regard to the difference in their medical condition. Also, the variables tested and compared in this study not only included the attenuation values of the image but also the image quality by testing the image noise and SNR.

This study also tested a method that has been believed helpful in decreasing the patient dose to prioritize the patient's safety by exposing the patient to the least amount of radiation needed to produce an image with an accurate diagnosis rate. By testing this method and finding that it was unable to replace the TNC image without decreasing the diagnostic ability of the scan, the patients were protected from a method that might expose them to higher radiation doses from repeated scans, or even face the danger of having their medical case being misdiagnosed.

5.6 Limitations of the Study

The limitations of this study include the fact that the images enrolled in the study were taken from the same institution and done on the same spectral CT scanner, which is the only spectral scanner in Palestine, if the images were taken from multiple scanners, it will reduce the bias created from the possibility of an error in the scanner or the institution's imaging protocol.

Although all the patients that were imaged using the scanner were enrolled in the study, the study sample was not large; to help generalize the study to the whole population, enrolling other patients from different institutions and medical centers could be helpful.

Another limitation that this study has faced is the lack of subjective image analysis that should be conducted by a radiologist, since having the radiologist rate the VNC images' quality will help test their diagnostic ability, and compare it with the TNC images' diagnostic ability. Also, during the objective image analysis, the attenuation values and the SNR of the images were the only variables studied; it would have made the results of the study stronger if the CNR and DLP were recorded and compared as well.

Additionally, the DLP that was collected in this study was the total DLP and not an individual DLP for each acquisition to help calculate the percentage and the amount of dose reduced from having the VNC image replace the TNC image.

And lastly, the ROIs that were placed in different regions in the images were only consisted in terms of their size in the same region for the same patient between the three images, but their sizes differ between images for different patients, and that can affect the comparison process.

5.7 Future Work

To help bring an understanding regarding VNC images and their ability to replace TNC images, future studies should focus on including multiple medical imaging centers in the study, and try to test the feasibility of using VNC images in particular medical cases and conditions, since VNC images might be more helpful for certain organs and tissues than others, or it could help with medical cases that do not require accurate attenuation values measurements. Future work should also include the radiologist's subjective rating of the image quality as it holds an important value when comparing the diagnosis ability of the image.

Furthermore, spectral CT scanners should be studied more to test the ability of the images created by material decomposition alongside VNC images in certain medical conditions, images such as bone removal, perfused blood image, atherosclerotic plaques removal, and VMI, should be studied thoroughly to determine the extent of their utility to improve CT images' potential in the medical field.

References

Abdulkareem, N.K. *et al.* (2023) 'Investigating the slice thickness effect on noise and diagnostic content of single-source multi-slice computerized axial tomography', *Journal of Medicine and Life*, 16(6), pp. 862–867. doi:10.25122/jml-2022-0188.

Al-Hayek, Y. *et al.* (2022) 'The reliability of CT numbers as absolute values for diagnostic scanning, dental imaging, and radiation therapy simulation: A narrative review', *Journal of Medical Imaging and Radiation Sciences*, 53(1), pp. 138–146. doi:10.1016/j.jmir.2021.11.007.

Anam, C. (2020) 'Noise Reduction in CT Images Using a Selective Mean Filter', *Journal of Biomedical Physics and Engineering*, 10(5). doi:10.31661/jbpe.v0i0.2002-1072.

Ananthakrishnan, L. *et al.* (2017) 'Spectral detector CT-derived virtual non-contrast images: comparison of attenuation values with unenhanced CT', *Abdominal Radiology*, 42(3), pp. 702–709. doi:10.1007/s00261-016-1036-9.

Brenner, D.J. *et al.* (2003) 'Cancer risks attributable to low doses of ionizing radiation: Assessing what we really know', *Proceedings of the National Academy of Sciences*, 100(24), pp. 13761–13766. doi:10.1073/pnas.2235592100.

Cao, G. *et al.* (2019) 'Reduced artifacts and improved diagnostic value of 640-slice computed tomography in patients with cardiac pacemakers', *Journal of International Medical Research*, 47(5), pp. 1916–1926. doi:10.1177/0300060519825986.

Chae, E.J. *et al.* (2010) 'Dual-energy Computed Tomography Characterization of Solitary Pulmonary Nodules', *Journal of Thoracic Imaging*, 25(4), pp. 301–310. doi:10.1097/RTI.0b013e3181e16232.

Costa, N. (2004) 'Understanding Contrast Media', *Journal of Infusion Nursing*, 27(5), pp. 302–312. doi:10.1097/00129804-200409000-00004.

Diwakar, M. and Kumar, M. (2018) 'A review on CT image noise and its denoising', *Biomedical Signal Processing and Control*, 42, pp. 73–88. doi:10.1016/j.bspc.2018.01.010.

Dundamadappa, S. *et al.* (2021) 'Multiphase CT Angiography: A Useful Technique in Acute Stroke Imaging—Collaterals and Beyond', *American Journal of Neuroradiology*, 42(2), pp. 221–227. doi:10.3174/ajnr.A6889.

Esquivel, A. *et al.* (2022) 'Photon-Counting Detector CT: Key Points Radiologists Should Know', *Korean Journal of Radiology*, 23(9), p. 854. doi:10.3348/kjr.2022.0377.

Fani, F. *et al.* (2014) 'CT-based thermometry: An overview', *International Journal of Hyperthermia*, 30(4), pp. 219–227. doi:10.3109/02656736.2014.922221.

Foley, W.D. *et al.* (2000) 'Multiphase Hepatic CT with a Multirow Detector CT Scanner', *American Journal of Roentgenology*, 175(3), pp. 679–685.

doi:10.2214/ajr.175.3.1750679.

Fornaro, J. *et al.* (2011) 'Dual- and multi-energy CT: approach to functional imaging', *Insights into Imaging*, 2(2), pp. 149–159. doi:10.1007/s13244-010-0057-0.

Garnett, R. (2020) 'A comprehensive review of dual-energy and multi-spectral computed tomography', *Clinical Imaging*, 67, pp. 160–169. doi:10.1016/j.clinimag.2020.07.030.

Graser, A. *et al.* (2006) 'Dose Reduction and Image Quality in MDCT Colonography Using Tube Current Modulation', *American Journal of Roentgenology*, 187(3), pp. 695–701. doi:10.2214/AJR.05.0662.

Greffier, J. *et al.* (2020) 'Effect of tin filter-based spectral shaping CT on image quality and radiation dose for routine use on ultralow-dose CT protocols: A phantom study', *Diagnostic and Interventional Imaging*, 101(6), pp. 373–381. doi:10.1016/j.diii.2020.01.002.

Hagen, C.K. *et al.* (2020) 'Cycloidal Computed Tomography', *Physical Review Applied*, 14(1), p. 014069. doi:10.1103/PhysRevApplied.14.014069.

Hara, A.K. *et al.* (2013) 'Reducing Body CT Radiation Dose: Beyond Just Changing the Numbers', *American Journal of Roentgenology*, 201(1), pp. 33–40. doi:10.2214/AJR.13.10556.

Hong, Y. *et al.* (2023) 'Application of spectral CT in diagnosis, classification and prognostic monitoring of gastrointestinal cancers: progress, limitations and prospects', *Frontiers in Molecular Biosciences*, 10. doi:10.3389/fmolb.2023.1284549.

Hua, C. *et al.* (2018) 'Accuracy of electron density, effective atomic number, and iodine concentration determination with a dual-layer dual-energy computed tomography system', *Medical Physics*, 45(6), pp. 2486–2497. doi:10.1002/mp.12903.

Hunter, N. and Muirhead, C.R. (2009) 'Review of relative biological effectiveness dependence on linear energy transfer for low-LET radiations', *Journal of Radiological Protection*, 29(1), pp. 5–21. doi:10.1088/0952-4746/29/1/R01.

Jamali, S. *et al.* (2019) 'Virtual unenhanced phase with spectral dual-energy CT: Is it an alternative to conventional true unenhanced phase for abdominal tissues?', *Diagnostic and Interventional Imaging*, 100(9), pp. 503–511. doi:10.1016/j.diii.2019.04.007.

Javadi, S. *et al.* (2020) 'Quantitative attenuation accuracy of virtual non-enhanced imaging compared to that of true non-enhanced imaging on dual-source dual-energy CT', *Abdominal Radiology*, 45(4), pp. 1100–1109. doi:10.1007/s00261-020-02415-8.

Johnson, T.R.C. *et al.* (2007) 'Material differentiation by dual energy CT: initial experience', *European Radiology*, 17(6), pp. 1510–1517. doi:10.1007/s00330-006-0517-6.

Johnson, T.R.C. (2012) 'Dual-Energy CT: General Principles', *American Journal of Roentgenology*, 199(5_supplement), pp. 3–8. doi:10.2214/AJR.12.9116.

Kapoor, V., McCook, B.M. and Torok, F.S. (2004) 'An Introduction to PET-CT Imaging', *RadioGraphics*, 24(2), pp. 523–543. doi:10.1148/rg.242025724.

Kaufmann, S. *et al.* (2013) 'Tin-filter Enhanced Dual-Energy-CT', *Academic Radiology*, 20(5), pp. 596–603. doi:10.1016/j.acra.2013.01.010.

Kelly, J. *et al.* (1989) 'The value of non-contrast-enhanced CT in blunt abdominal trauma', *American Journal of Roentgenology*, 152(1), pp. 41–48. doi:10.2214/ajr.152.1.41.

Laukamp, K.R. *et al.* (2020) 'Virtual non-contrast for evaluation of liver parenchyma and vessels: results from 25 patients using multi-phase spectral-detector CT', *Acta Radiologica*, 61(8), pp. 1143–1152. doi:10.1177/0284185119893094.

Lee, J.S. *et al.* (2023) 'Comparison of True and Virtual Non-Contrast Images of Liver Obtained with Single-Source Twin Beam and Dual-Source Dual-Energy CT', *Journal of the Korean Society of Radiology*, 84(1), p. 170. doi:10.3348/jksr.2021.0193.

Lehti, L. *et al.* (2019) 'Comparing Arterial- and Venous-Phase Acquisition for Optimization of Virtual Noncontrast Images From Dual-Energy Computed Tomography Angiography', *Journal of Computer Assisted Tomography*, 43(5), pp. 770–774. doi:10.1097/RCT.0000000000000903.

Li, P.-H. *et al.* (2018) 'The Role of Noncontrast CT in the Evaluation of Surgical Abdomen Patients', *The American Surgeon*, 84(6), pp. 1015–1021. doi:10.1177/000313481808400658.

Lin, Y.-M. *et al.* (2018) 'Attenuation values of renal parenchyma in virtual noncontrast images acquired from multiphase renal dual-energy CT: Comparison with standard noncontrast CT', *European Journal of Radiology*, 101, pp. 103–110. doi:10.1016/j.ejrad.2018.02.001.

Marin, D. *et al.* (2011) 'Body CT: Technical Advances for Improving Safety', *American Journal of Roentgenology*, 197(1), pp. 33–41. doi:10.2214/AJR.11.6755.

McCollough, C.H. *et al.* (2009) 'Strategies for Reducing Radiation Dose in CT', *Radiologic Clinics of North America*, 47(1), pp. 27–40. doi:10.1016/j.rcl.2008.10.006.

McCollough, C.H. *et al.* (2015) 'Dual- and Multi-Energy CT: Principles, Technical Approaches, and Clinical Applications', *Radiology*, 276(3), pp. 637–653. doi:10.1148/radiol.2015142631.

Meloni, A. *et al.* (2024) 'Spectral Photon-Counting Computed Tomography: Technical Principles and Applications in the Assessment of Cardiovascular Diseases', *Journal of Clinical Medicine*, 13(8), p. 2359. doi:10.3390/jcm13082359.

Menon, B.K. *et al.* (2015) 'Multiphase CT Angiography: A New Tool for the Imaging Triage of Patients with Acute Ischemic Stroke', *Radiology*, 275(2), pp. 510–520. doi:10.1148/radiol.15142256.

Mohammadinejad, P. *et al.* (2021) 'CT Noise-Reduction Methods for Lower-Dose

Scanning: Strengths and Weaknesses of Iterative Reconstruction Algorithms and New Techniques', *RadioGraphics*, 41(5), pp. 1493–1508. doi:10.1148/rg.2021200196.

Mussa, F.F. *et al.* (2016) 'Acute Aortic Dissection and Intramural Hematoma', *The Journal of American Medical Association*, 316(7), p. 754. doi:10.1001/jama.2016.10026.

Payor, A. *et al.* (2015) 'Efficacy of Noncontrast Computed Tomography of the Abdomen and Pelvis for Evaluating Nontraumatic Acute Abdominal Pain in the Emergency Department', *The Journal of Emergency Medicine*, 49(6), pp. 886–892. doi:10.1016/j.jemermed.2015.06.062.

Rassouli, N. *et al.* (2017) 'Detector-based spectral CT with a novel dual-layer technology: principles and applications', *Insights into Imaging*, 8(6), pp. 589–598. doi:10.1007/s13244-017-0571-4.

Roman, A. *et al.* (2018) 'CT-guided procedures: an initial experience', *Medicine and Pharmacy Reports*, 91(4), pp. 427–434. doi:10.15386/cjmed-1145.

Salyapongse, A.M. and Szczykutowicz, T.P. (2024) 'Misinterpretations about CT numbers, material decomposition, and elemental quantification', *European Radiology* [Preprint]. doi:10.1007/s00330-024-10934-x.

Sauter, A.P. *et al.* (2018) 'Dual-layer spectral computed tomography: Virtual non-contrast in comparison to true non-contrast images', *European Journal of Radiology*, 104, pp. 108–114. doi:10.1016/j.ejrad.2018.05.007.

Schena, E. *et al.* (2015) 'Emerging clinical applications of computed tomography', *Medical Devices: Evidence and Research*, p. 265. doi:10.2147/MDER.S70630.

Schöckel, L. *et al.* (2020) 'Developments in X-Ray Contrast Media and the Potential Impact on Computed Tomography', *Investigative Radiology*, 55(9), pp. 592–597. doi:10.1097/RLI.0000000000000696.

Schulz, R.A., Stein, J.A. and Pelc, N.J. (2021) 'How CT happened: the early development of medical computed tomography', *Journal of Medical Imaging*, 8(05). doi:10.1117/1.JMI.8.5.052110.

Seeram, E. and Sil, J. (2013) 'Computed Tomography: Physical Principles, Instrumentation, and Quality Control', in *Practical SPECT/CT in Nuclear Medicine*. London: Springer London, pp. 77–107. doi:10.1007/978-1-4471-4703-9_5.

Shah, D.J., Sachs, R.K. and Wilson, D.J. (2012) 'Radiation-induced cancer: a modern view', *The British Journal of Radiology*, 85(1020), pp. 1166–1173. doi:10.1259/bjr/25026140.

Si-Mohamed, S. *et al.* (2019) 'Virtual versus true non-contrast dual-energy CT imaging for the diagnosis of aortic intramural hematoma', *European Radiology*, 29(12), pp. 6762–6771. doi:10.1007/s00330-019-06322-5.

Siegel, M.J., Bhalla, S. and Cullinane, M. (2021) 'Dual-Energy CT Material

Decomposition in Pediatric Thoracic Oncology', *Radiology: Imaging Cancer*, 3(1), p. e200097. doi:10.1148/rycan.2021200097.

Slebocki, K. *et al.* (2017) 'Incidental Findings in Abdominal Dual-Energy Computed Tomography', *Journal of Computer Assisted Tomography*, 41(2), pp. 294–297. doi:10.1097/RCT.0000000000000503.

Smith-Bindman, R. (2009) 'Radiation Dose Associated With Common Computed Tomography Examinations and the Associated Lifetime Attributable Risk of Cancer', *Archives of Internal Medicine*, 169(22), p. 2078. doi:10.1001/archinternmed.2009.427.

So, A. and Nicolaou, S. (2021) 'Spectral Computed Tomography: Fundamental Principles and Recent Developments', *Korean Journal of Radiology*, 22(1), p. 86. doi:10.3348/kjr.2020.0144.

Sommer, C.M. *et al.* (2012) 'Iodine removal in intravenous dual-energy CT-cholangiography: Is virtual non-enhanced imaging effective to replace true non-enhanced imaging?', *European Journal of Radiology*, 81(4), pp. 692–699. doi:10.1016/j.ejrad.2011.01.087.

Stiller, W. (2018) 'Basics of iterative reconstruction methods in computed tomography: A vendor-independent overview', *European Journal of Radiology*, 109, pp. 147–154. doi:10.1016/j.ejrad.2018.10.025.

Stolzmann, P. *et al.* (2008) 'Endoleaks after Endovascular Abdominal Aortic Aneurysm Repair: Detection with Dual-Energy Dual-Source CT', *Radiology*, 249(2), pp. 682–691. doi:10.1148/radiol.2483080193.

Sulieman, A. *et al.* (2022) 'Effective radiation dose and radiogenic cancer risk during contrast enhanced abdominal computed tomography examinations', *Radiation Physics and Chemistry*, 200, p. 110328. doi:10.1016/j.radphyschem.2022.110328.

Takahashi, Y. *et al.* (2018) 'Image quality and radiation dose of low-tube-voltage CT with reduced contrast media for right adrenal vein imaging', *European Journal of Radiology*, 98, pp. 150–157. doi:10.1016/j.ejrad.2017.11.017.

Tapfer, A. *et al.* (2012) 'Experimental results from a preclinical X-ray phase-contrast CT scanner', *Proceedings of the National Academy of Sciences*, 109(39), pp. 15691–15696. doi:10.1073/pnas.1207503109.

Tian, S.-F. *et al.* (2015) 'Application of Computed Tomography Virtual Noncontrast Spectral Imaging in Evaluation of Hepatic Metastases', *Chinese Medical Journal*, 128(5), pp. 610–614. doi:10.4103/0366-6999.151656.

Toepker, M. *et al.* (2012) 'Virtual non-contrast in second-generation, dual-energy computed tomography: Reliability of attenuation values', *European Journal of Radiology*, 81(3), pp. 398–405. doi:10.1016/j.ejrad.2011.12.011.

Wang, J. *et al.* (2021) 'Value of multiphase contrast-enhanced CT with three-dimensional reconstruction in detecting depth of infiltration, lymph node metastasis, and

extramural vascular invasion of gastric cancer', *Journal of Gastrointestinal Oncology*, 12(4), pp. 1351–1362. doi:10.21037/jgo-21-276.

Yoo, S.Y. *et al.* (2013) 'Dual-Energy CT in the Assessment of Mediastinal Lymph Nodes: Comparative Study of Virtual Non-Contrast and True Non-Contrast Images', *Korean Journal of Radiology*, 14(3), p. 532. doi:10.3348/kjr.2013.14.3.532.

Zhang, R. *et al.* (2018) 'Quantitative accuracy of CT numbers: Theoretical analyses and experimental studies', *Medical Physics*, 45(10), pp. 4519–4528. doi:10.1002/mp.13119.

Zhao, H. (2003) 'Role of multiphase scans by multirow-detector helical CT in detecting small hepatocellular carcinoma', *World Journal of Gastroenterology*, 9(10), p. 2198. doi:10.3748/wjg.v9.i10.2198.

Appendices

Appendix A: IRB Approval Letter

Arab American University
Institutional Review Board - Ramallah

الجامعة العربية الأمريكية
مجلس اخلاقيات البحث العلمي – رام الله

IRB Approval Letter

Study Title: "Comparing Arterial Virtual Non-Contrast Scans with Venous Virtual Non-Contrast Scans in their Feasibility to Substitute True Non-Contrast Scans Using Detector-Based Spectral Computed Tomography Scanner".

Submitted by: Manar Mohammad Mahmoud Qaisi

Date received: 6th January 2024

Date reviewed: 1st February 2024

Date approved: 29th July 2024

Your Study titled **"Comparing Arterial Virtual Non-Contrast Scans with Venous Virtual Non-Contrast Scans in their Feasibility to Substitute True Non-Contrast Scans Using Detector-Based Spectral Computed Tomography Scanner"** with the code number **"R-2024/A/125/N"** was reviewed by the Arab American University Institutional Review Board - Ramallah and it was approved on the 29th of July 2024.

Sajed Ghawadra, PhD
IRB-R Chairman
Arab American University of Palestine

الجامعة العربية الأمريكية - فلسطين
مجلس اخلاقيات البحث العلمي - رام الله
IRB-R
ARAB AMERICAN UNIVERSITY-PALESTINE
INSTITUTIONAL REVIEW BOARD - RAMALLAH

General Conditions:

1. Valid for 6 months from the date of approval.
2. It is important to inform the IRB-R with any modification of the approved study protocol.
3. The Bord appreciates a copy of the research when accomplished.

رام الله – فلسطين

Tel: 02-294-1999 **E-Email:** IRB-R@aaup.edu **Website:** www.aaup.edu

Appendix B: AAUP Approval

2024/8/20

السادة في مستوصف الرحمة/نابلس المحترمين

تسهيل مهمة بحثية

تحية طيبة وبعد،

تُهديكم كلية الدراسات العليا في الجامعة العربية الأمريكية أطيب التحيات، وبالإشارة الى الموضوع أعلاه، تشهد كلية الدراسات العليا في الجامعة أن الطالبة **منار محمد محمود القيسي** والتي تحمل الرقم الجامعي 202113094هي طالبة ماجستير في برنامج التصوير الطبقي والرنين المغناطيسي وتعمل على رسالة الماجستير الخاصة بها بعنوان:

" مقارنة صور الطبقية الغير الملونة الافتراضية المأخوذة من مرحلة تصوير الوريد بالصور المأخوذة من مرحلة تصوير الشريان بقابلية استبدال الصور الغير ملونة الحقيقية بهما باستخدام الجهاز الطبقي الطيفي المبني على كاشف الجهاز"، تحت إشراف الدكتور عبد السلام خلف. نأمل من حضرتكم الإيعاز لمن يلزم لمساعدتها للحصول على المعلومات اللازمة للدراسة علماً أن المعلومات ستستخدم لغاية البحث فقط وسيتم التعامل معها بغاية السرية، وقد أُعطيت هذه الرسالة بناءً على طلبها.

وتفضلوا بقبول فائق الاحترام

عميد كلية الدراسات العليا

د. نوار قطب

كلية الدراسات العليا
FACULTY OF GRADUATE STUDIES

Jenin Tel: +970-4-2418888 Ext.:1471,1472 Fax: +970-4-2510810 P.O. Box:240
Ramallah Tel: +970-2-2941999 Fax: +970-2-2941979 Abu Qash - Near Alrehan
E-mail: FGS@aaup.edu ; PGS@aaup.edu Website: www.aaup.edu

Appendix C: Data Collection Form

	TNC		VNC-A		VNC-V	
	MA	SD	MA	SD	MA	SD
ROI(1)						
ROI(2)						
ROI(3)						
ROI(4)						
ROI(5)						

Age: _____ years Gender:_____ DLP: _____

(ROI (1): aorta at the level of the diaphragm / (2): aorta at the level of renal arteries/ (3): within the right lobe of the liver/ (4): retroperitoneal fat/ (5): psoas muscle.)

مقارنة صور الطبقية الغير الملونة الافتراضية المأخوذة من مرحلة تصوير الوريد بالصور الماخوذة من مرحلة تصوير الشريان بقابلية استبدال الصور الغير ملونة الحقيقية بهما باستخدام الجهاز الطبقي الطيفي المبني على كاشف الجهاز

منار محمد محمود القيسي

لجنة الاشراف

د. عبد السلام احمد خلف

د. أحمد رفيق أبو عرة

د. أسامة علي خدرج

ملخص

المقدمة: يعد جهاز التصوير الطبقي الطيفي من أحد الابتكارات في علم التصوير التي ساعدت تقليل جرعة الأشعة لدى المريض وتحسين جودة الصورة, أحد التطبيقات التي يمكن القيام بها باستخدام التصوير الطبقي الطيفي هي انشاء الصور الطبقية الغير ملونة الافتراضية عن طريق خوارزمية تحليل المواد, هذه الصور يمكن انشائها من أي مرحلة من التصوير الملون. في حال كانت الصور الافتراضية الغير ملونة مشابهة كفاية للصور الغير ملونة الحقيقية, فيمكن استبدال الصور الحقيقية بالصور الافتراضية وتقليل جرعة الأشعة للمريض.

الهدف: هذه الدراسة تهدف الى مقارنة الصور الافتراضية الغير ملونة المأخوذة من مرحلة تصوير الوريد

والصور الغير ملونة الافتراضية المأخوذة من مرحلة تصوير الشريان بالصور الغير ملونة الحقيقية لمنطقة البطن, من اجل تحديد اذا كانت احداهما مشابهة كفاية للصور الغير ملونة الحقيقية لاستبدالها.

الطريقة: 141 فحص مقطعي للبطن تم عملهم في مستوصف الرحمة ما بين شهر تموز سنة 2022 وشهر تشرين الاول سنة 2024 باستخدام الجهاز الطبقي الطيفي المبني على كاشف الجهاز, تم تسجيلهم في الدراسة, كل فحص كان يشمل صورة غير ملونة, صورة ملونة للمرحلة الوريدية, وصورة ملونة للمرحلة الشريانية. تم انشاء صور افتراضية غير ملونة من المرحلتين الشريانية والوريدية الملونتين, وتم مقارنة الصور بناءا على المتوسط الحسابي والانحراف المعياري داخل مناطق اهتمام محددة الموجودة في خمس اماكن داخل البطن, من اجل اظهار الاختلافات بين الصور بناءا على المتوسط لقيم التوهين وضوضاء الصورة.

النتيجة: العلاقة بين الصور الغير ملونة الحقيقية والصور الغير ملونة الافتراضية المأخوذة من مرحلة تصوير الوريد, والعلاقة بين الصور الغير ملونة الحقيقية والصور الغير ملونة الافتراضية المأخوذة من مرحلة تصوير الشريان داخل جميع مناطق الاهتمام كانت مختلفة بشكل كبير وبارز, الصور الغير ملونة الحقيقية كان متوسطها الحسابي والانحراف المعياري الخاص فيها أعلى من تلك لدى الصور الافتراضية من النوعين (46.36 المتوسط الحسابي للصورة الحقيقية مقارنة بصورة الوريد الافتراضية (39.87) وصورة الشريان الافتراضية (34.66) في منطقة الاهتمام الثانية, 19.27 الانحراف المعياري للصورة الحقيقية مقارنة بصورة الوريد الافتراضية (10.45) وصورة الشريان الافتراضية (10.34) في منطقة الاهتمام الخامسة). نسبة الاشارة الى الضوضاء في الصور الغير ملونة الحقيقية كانت أيضا أعلى من تلك للصور الافتراضية.

الاستنتاج: لم يكن أي من الصور الافتراضية الغير ملونة المأخوذة من مرحلة الشرايين او مرحلة الوريد كافية لاستبدال الصور الغير ملونة الحقيقية من دون انزال جودة الصورة وامكانيتها في التشخيص بسبب الاختلاف البارز في قيم الوسط الحسابي ونسبة الاشارة الى الضوضاء.

الكلمات المفتاحية: التصوير الطبقي الطيفي, الصور الافتراضية الغير ملونة, الصور الحقيقية الغير ملونة, الصور الغير ملونة الافتراضية الماخوذة من مرحلة الوريد, الصور الغير ملونة الافتراضية الماخوذة من مرحلة الشريان.